UAV-Enabled Data Collection Over Clustered Machine-Type Communication Networks: AEM Modeling and Trajectory Planning

Lingfeng Shen, Ning Wang, *Member, IEEE*, Zhengyu Zhu, *Senior Member, IEEE*, Wei Xu, *Senior Member, IEEE*, Yue Li, Xiaomin Mu, and Lin Cai, *Fellow, IEEE*

***Abstract*—Machine-type communications (MTC) is a key technology for Internet-of-Things (IoT) services in 5G mobile communications and beyond. An essential design problem for an MTC network is the efficient and scalable data collection from low-power machine-type communication devices (MTCDs). This paper uses unmanned aerial vehicles (UAVs) to facilitate data collection from a clustered MTC network on the ground. The notion of artificial energy map (AEM) is introduced as a novel modeling technique for energy efficiency analysis, which is critical to the subject of investigation here considering the limited energy of battery-powered MTCDs and UAVs. The proposed design framework first determines the number of MTCD clusters L_{opt} according to a certain criterion. A greedy learning clustering (GLC) algorithm is then employed to divide the MTCDs into L_{opt} clusters. For each MTCD cluster, an AEM is constructed, and the optimal UAV hovering strategy within the cluster can be obtained accordingly. Finally, the UAV stations travel across the clusters and collect data from each cluster while hovering above it. This AEM-based modeling technique leads to a solution that can effectively improve the energy efficiency (EE) of UAV-enabled data collection. However, the MTCD clustering strategy, UAV hovering strategy, and UAV flying strategy all have impacts on the overall energy efficiency, which results in a coupled optimization problem that is difficult to solve. The GLC-AEM method is proposed to decouple the original EE optimization problem into sub-problems that can be handled easily by standard optimization techniques. Simulation results show that the GLC-AEM algorithm can be applied to UAV-enabled data collection scenarios with single and multiple UAV stations, and it can improve the overall EE effectively. Besides, the GLC-AEM algorithm shows good scalability and consistent performance in clustered MTC networks. The more MTCDs, the higher the achieved EE.**

***Index Terms*—Artificial energy map, clustered MTC network, energy efficiency, trajectory planning, UAV-enabled data collection.**

Manuscript received 17 September 2021; revised 2 March 2022; accepted 18 May 2022. Date of publication 9 June 2022; date of current version 19 September 2022. Preliminary results of this work have been presented in the *2020 IEEE International Conference on Communications (ICC 2020)*. The review of this article was coordinated by Prof. Jun Won Choi. *(Corresponding author: Ning Wang.)*

Lingfeng Shen, Ning Wang, Zhengyu Zhu, and Xiaomin Mu are with the School of Information Engineering, Zhengzhou University, Zhengzhou 450001, China (e-mail: ielfshen@163.com; ienwang@zzu.edu.cn; iezyzhu@zzu.edu.cn; iexmmu@zzu.edu.cn).

Wei Xu is with the School of Information Science and Engineering, Southeast University, Nanjing 210096, China (e-mail: wxu@seu.edu.cn).

Yue Li and Lin Cai are with the Department of Electrical and Computer Engineering, University of Victoria, Victoria, BC V8W 3P6, Canada (e-mail: liyue331@uvic.ca; cai@ece.uvic.ca).

Digital Object Identifier 10.1109/TVT.2022.3181158

I. Introduction

MASSIVE machine-type communication (mMTC) is an important use case of Internet-of-Things (IoT) applications in 5G, which has attracted a lot of research interests in recent years [1]–[4]. Because of its broad coverage and large connectivity, the mMTC network is the key enabler of scaling up emerging IoT services such as environmental monitoring, forest fire prevention, smart healthcare, etc. Achieving highly efficient data collection from a huge number of low-cost, low-complexity machine-type communication devices (MTCDs) is one key issue that must be addressed for mMTC networks. However, supporting access of massive MTCDs with high dynamics and broad distribution requires significant resources and infrastructure, which poses great challenges to legacy cellular networking [5]–[7].

Evolutional amendments to legacy cellular standards have been proposed for cellular IoT services [8], which have partly addressed the issues with providing scalable services to MTCDs. To better support mMTC, as well as ultra-reliable low-latency communication (uRLLC) applications, new disruptive technologies have to be introduced to the radio access network (RAN). Recently, unmanned aerial vehicles (UAVs) have been exploited as a promising airborne communication platform [9]–[11]. Due to their mobility, hovering, low-cost and flexible deployment features, UAVs have great potentials in providing communication services to remote and disaster-strike areas [13]–[15], [31]. It is a promising solution to mMTC applications, especially when efficiency is the key consideration while latency requirement is relaxed [16]–[18]. Specifically, the UAV stations can approach the MTCDs and exploit the favorable line-of-sight (LoS) communication links for efficient data transmission.

There has been an extensive focus on the task completion time and the age of information (AoI) for UAV-assisted data collection. In [19], minimization of the data collection time was achieved by jointly optimizing the UAV's trajectory and transmission scheduling of the ground MTCD nodes. A mixed-integer nonlinear programming (MINLP) problem was formulated, and a solution technique based on successive convex optimization was proposed. The notion of average AoI of ground-based sensors transmitting data to a UAV station was introduced and minimized in [20]. The UAV was used as a mobile data collector as well as an energy source transferring energy to the ground-based sensor nodes. A problem that

0018-9545 © 2022 IEEE. Personal use is permitted, but republication/redistribution requires IEEE permission.
See https://www.ieee.org/publications/rights/index.html for more information.

Authorized licensed use limited to: UNIVERSITY OF VICTORIA. Downloaded on January 26,2023 at 04:32:29 UTC from IEEE Xplore. Restrictions apply.

jointly optimizes the UAV's trajectory, the sensor nodes' energy harvesting and data transmission time was formulated and solved accordingly. Consider that it is challenging to collect data from massive MTCDs while ensuring the freshness of information with one single UAV station, the problem of AoI-optimal data collection enabled by multiple UAVs under energy constraints was studied [21]. Similarly, completion time minimization for multi-UAV-enabled data collection in wireless sensor networks (WSNs) was investigated in [22].

Due to the low-power, low-complexity nature of the MTCDs, energy efficiency (EE) is important performance measure for machine-type communications. As mentioned above, when the EE requirement outweighs the latency requirement, using UAVs to collect data is promising for mMTC applications. In [23], the trade-off between overall throughput and energy consumption of UAV-IoT systems was investigated. A novel UAV-assisted IoT network was studied in [24]. In addition to being a mobile data collector, the UAV platform was also used as an airborne anchor node to assist 3D positioning of the IoT devices. By jointly optimizing the UAV's flight trajectory and transmission scheduling, the energy consumption was minimized, subject to the communication reliability and positioning accuracy constraints. To maximize the energy efficiency for data collection, a UAV-assisted backscatter communication scheme was studied in [25]. A closed-form expression for average outage probability was derived to determine the optimal UAV data collection location. Recently, a UAV-assisted wireless sensor network with wireless charging was studied in [26]. The ground-based sensors are divided into multiple groups. A Markov decision problem was formulation, and a Q-learning solution approach using a new reward function was proposed, which hit a good balance between average throughput, delay, and energy efficiency.

In UAV-enabled data collection over clustered mMTC networks, clustering strategies, transmission scheduling, UAVs' deployment, and trajectory optimization significantly impact data collection EE. Existing works have their advantages, but to our best knowledge, there is no sound system modeling that can comprehensively consider the balance between the EE, transmission delay, and the system's scalability. In this paper, we study an energy-efficient and scalable UAV-enabled data collection scheme for mMTC networks. A new modeling technique is proposed to design the MTCDs' clustering strategy, UAVs' flying and hovering strategies. The impact of system expansion on data collection EE and delay has been investigated, including the extension from single UAV to multiple UAVs and the extension of system scale. Specifically, a modeling technique based on the notion of artificial energy map (AEM) is proposed to characterize the system from the EE perspective. To efficiently serve a large number of MTCDs, a greedy learning clustering (GLC) scheme based on a certain criterion is proposed to divide the target MTCDs into clusters. A GLC-AEM algorithm for efficient data collection in the large-scale and high-density mMTC scenario is proposed and its performance is evaluated subsequently. The main contributions of this work are summarized in the following.

- The AEM is proposed as a new modeling technique for UAV-enabled data collection in mMTC networks. This model describes the single-UAV, delay-insensitive data collection system from the energy efficiency perspective, and it can also be extended to multi-UAV scenarios.
- To improve data collection efficiency, an mMTC network to be served is divided into cluster. A clustering number determining (CND) algorithm finds the optimal number of clusters $L_{\rm opt}$ according to certain principle. Two principles, namely clustering principle I (CP-I) and clustering principle II (CP-II) are studied for the CND algorithm design. Specifically, CP-I minimizes the number of clusters subject to the UAV's service radius and service capacity constraints, while CP-II minimizes the maximum cluster radius $r_{\max}$.
- Based on the optimal number of clusters $L_{\rm opt}$ determined by the CND algorithm, the GLC scheme is proposed to group the MTCDs in the mMTC network into $L_{\rm opt}$ clusters according to the channel state information (CSI) and the task properties.
- The problem of minimizing the energy consumption through UAV trajectory design is formulated. The problem exhibits strong coupling between the clustering strategy, the UAV hovering strategy, as well as the UAV flying route. The GLC-AEM scheme is proposed to decouple the original problem, which is shown to achieve good energy efficiency with low complexity.

The remainder of this paper is organized as follows. The system model under investigation and the original optimization problem formulation are presented in Section II. The novel AEM modeling technique is proposed in Section III. The GLC-AEM algorithm for clustering and UAV hovering strategy design is proposed subsequently in Section IV. The complexity of the proposed algorithm is analyzed in Section V. Numerical results that evaluate the performance of the proposed schemes are presented in Section VI. Concluding remarks are given in Section VII.

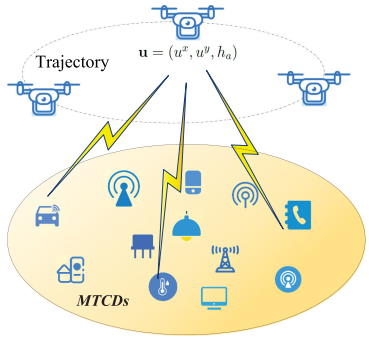

Fig. 1. The UAV-enabled data collection system model.

II. System Model and Problem Description

In this work, we consider a UAV-enabled data collection system for mMTC scenario, as shown in Fig. 1. A large number of MTCDs are distributed on the ground. The UAV collects data from the MTCDs while flying over the target service area. By optimizing the UAV's trajectory, the energy consumption of this system is minimized subject to completion of the data collection

Authorized licensed use limited to: UNIVERSITY OF VICTORIA. Downloaded on January 26,2023 at 04:32:29 UTC from IEEE Xplore. Restrictions apply.

TABLE I
TABLE OF NOTATIONS

Notation	Physical Meaning
$K, \mathcal{K}$	MTCD Number and MTCD set
$K_l, \mathcal{K}_l$	MTCD Number and MTCD set in cluster l
$P_k, P_{\max}$	The transmitting power and its upper limit
$\mathbf{q}_k, \mathbf{u}$	MTCD location and UAV location
$\mathbf{u}_s, \mathbf{u}_e$	Preset starting point and ending point
T, N, τ	The total flight time (s), number of time slots, and time slot length
a, b	The LoS occurrence probability parameters
$\mathbf{\Gamma}, \mathbf{\Delta}$	The UAV flying time and hovering time set
$S_{\min}, S_{\max}$	The cluster size parameter
ω_C, ω_M	Weighting parameters in the design objective
L	The number of clusters
h_k	The channel coefficients
β_k, $\tilde{h_k}$	Large- and small-scale fading coefficients
d_k	The Euclidean distance
θ	The elevation angle
E_{C}, E_{M}	The data transmission and UAV maneuvering energies
$r_{\max}$	The UAV's maximum service radius
v	Maximum UAV speed (m/s)
σ^2	Power of AWGN (dBm/Hz)
B	Communication bandwidth (Hz)
B_k	The data size (Mb)
m	The mass of UAV (kg)
r_p	The UAV's radius (cm)
n_p	The UAV's number of propellers
η_m, η_p	Motor and propeller efficiencies
β_0	The path loss (dB) at the reference distance
κ	NLoS additional attenuation factor
$\mathbf{Q}_k$	The communication power matrix

task. For convenience, the symbol notations used in this paper are summarized in Table I.

A. Data Collection Scenario and Channel Model

As shown in Fig. 1, we consider an mMTC network consisting of K ground-based MTCDs and one single UAV station. The MTCD set is denote as $\mathcal{K} = \{1, 2, \ldots, K\}$. The UAV flies at a constant speed v. Define the altitude of the ground as 0, and the flying altitude of the UAV as h_a. The location coordinates of the MTCDs and the UAV are expressed as $\mathbf{q}_k = (q_k^x, q_k^y, 0), k = 1, \ldots, K$ and $\mathbf{u} = (u^x, u^y, h_a)$, respectively.

Assume that the UAV station has all the MTCDs' position information in advance. The UAV flies from a preset starting point $\mathbf{u}_s = (u_s^x, u_s^y, h_a)$ to a preset ending point $\mathbf{u}_e = (u_e^x, u_e^y, h_a)$. It collects data from the MTCDs while flying over the service area. All the MTCDs have fixed data transmission tasks that should be completed before the UAV finishes its flight. The UAV's total flight time T is equally divided into N slots of duration $\tau = T/N$, where N is sufficiently large to give fine time resolution. As a result, each time slot τ corresponding to a trajectory anchor is small enough to guarantee approximately constant air-to-ground wireless channels within τ. The instantaneous time can be expressed as $t_n = n\tau, n = 1, \ldots, N$.

We use $h_k(t_n), k = 1, \ldots, K$, to denote the channel coefficient between the k^{th} MTCD and the UAV at time instance t_n. As in [27] and [28], $h_k(t_n)$ adopts the form

$$h_k(t_n) = \sqrt{\beta_k(t_n)}\tilde{h_k}(t_n), \tag{1}$$

where $\beta_k(t_n)$ characterizes the large-scale effects such as path-loss and shadowing, and $\tilde{h_k}(t_n)$ accounts for the small-scale fading. $\tilde{h_k}(t_n)$ is generally a complex-valued random variable with $\mathbb{E}[|\tilde{h_k}(t_n)|^2] = 1$. On the other hand, $\beta_k(t_n)$ takes different forms for LoS propagation and NLoS propagation, i.e.,

$$\beta_k(t_n) = \begin{cases} 1/\beta_0 d_k^2(t_n), & \text{LoS link} \\ \kappa/\beta_0 d_k^2(t_n), & \text{NLoS link} \end{cases} \tag{2}$$

where $d_k(t_n) = \|\mathbf{q}_k - \mathbf{u}(t_n)\|_2$ is the MTCD-UAV link distance, β_0 is the path-loss at the reference distance, and $\kappa < 1$ reflects the additional attenuation due to NLoS propagation.

At any time instance, either LoS or NLoS propagation occurs according to certain probabilistic model. In this work, we assume the probability of LoS propagation is given by

$$\Pr{}_{\mathrm{L}}(t_n) = \frac{1}{1 + a\exp(-b[\theta(t_n) - a])}, \tag{3}$$

where a, b are parameters determined by the radio propagation environment, and $\theta = \arcsin(\frac{h_a}{d})$ is the elevation angle. The probability of NLoS propagation is $\Pr{}_{\mathrm{NL}}(t_n) = 1 - \Pr{}_{\mathrm{L}}(t_n)$.

B. Energy Consumption Model

The overall energy consumption consists of two parts. The first is the data transmission energy consumption during the data collection process. The second is the UAV's maneuvering energy consumption.

1) Data Transmission Energy Consumption: Denote by $P_k(t_n)$ the instantaneous transmitting power of the k^{th} MTCD. Assume that the power consumption of the UAV receiver is a constant circuit power, which does not affect the optimization process. The energy consumption of the k^{th} MTCD for data transmission is $E_{k,\mathrm{C}} = \sum_{n=1}^{N} P_k(t_n)\tau$. The total data transmission energy is then given by

$$E_{\mathrm{C}} = \sum_{k=1}^{K} E_{k,\mathrm{C}}. \tag{4}$$

2) UAV Maneuvering Energy Consumption: As in [29], the UAV maneuvering energy consumption can be calculated as

$$E_{\mathrm{M}} = \sum_{n=1}^{N} \frac{m_{\mathrm{v}} g}{\eta_{\mathrm{m}}\eta_{\mathrm{p}}} v\tau, \tag{5}$$

where m_{v}, g are the mass of the UAV and the gravitation constant. η_{m} and η_{p} represent efficiency of the UAV's motor and propellers. v and τ represent the UAV's flying speed and flying time slot length.

Authorized licensed use limited to: UNIVERSITY OF VICTORIA. Downloaded on January 26,2023 at 04:32:29 UTC from IEEE Xplore. Restrictions apply.

C. Problem Formulation and the Global Optimal Trajectory

We next present the problem which maximizes the overall energy efficiency by optimizing the UAV's flying trajectory, subject to completion of the data collection tasks. Orthogonal radio resources, say different frequency bands, are assigned to different MTCDs for uplink transmissions to avoid inter-user interference. It is noted that if the UAV could finish the data collection tasks, the sum of the achievable rates must satisfy the following inequality for every MTCD.

$$\sum_{n=1}^{N} \mathbb{E}\left[B\log_2\left(1+\frac{P_k(t_n)|h_k(t_n)|^2}{\sigma^2}\right)\tau\right] \geq B_k,\ k=1,\ldots,K, \tag{6}$$

where B denotes the communication bandwidth in hertz (Hz) that is assigned to every MTCD. The left hand side (LHS) of (6) is the overall data throughput of the k^{th} MTCD over all N time slots. σ^2 denotes the additive white Gaussian noise (AWGN) power. B_k on the right hand side (RHS) is a quantity that reflects the data size of the k^{th} MTCD, and the unit of B_k is Mb.

Eqn. (6), as a constraint, is difficult to handle when optimizing the UAV trajectory for maximized energy efficiency. To circumvent this, a lower bounding technique is used to replace the LHS of (6). Define $\lambda_k(t_n) = 1/\beta_k(t_n)|\tilde{h_k}(t_n)|^2$, $\log_2(1+\frac{P_k(t_n)}{\lambda_k(t_n)\sigma^2})$ is a convex function of $\lambda_k(t_n)$. A lower bound of the expected throughput can be derived according to Jensen's inequality as

$$\begin{aligned}
&\mathbb{E}\left[B\log_2\left(1+\frac{P_k(t_n)|h_k(t_n)|^2}{\sigma^2}\right)\right]\\
&=\mathbb{E}\left[B\log_2\left(1+\frac{P_k(t_n)}{\lambda_k(t_n)\sigma^2}\right)\right]\\
&\geqslant B\log_2\left(1+\frac{P_k(t_n)}{\mathbb{E}[\lambda_k(t_n)]\sigma^2}\right)\\
&=B\log_2\left(1+\frac{P_k(t_n)(\Pr_{\mathrm{L}}(t_n)+(1-\Pr_{\mathrm{L}}(t_n))\kappa)}{\beta_0\sigma^2\|\mathbf{q}_k-\mathbf{u}(t_n)\|_2^2}\right)\triangleq \bar{R}(t_n).
\end{aligned} \tag{7}$$

The overall energy efficiency of the mMTC data collection system is given by $\frac{\sum_{k=1}^{K}B_k}{\omega_C E_C+\omega_M E_M}$, where ω_C and ω_M are adjustable weighting parameters. Since B_k is a constant, maximizing the energy efficiency is equivalent to minimizing the overall energy consumption. The UAV trajectory and MTCD transmit power optimization problem is then formulated as

$$\mathbf{P0}: \underset{\{u^x(t_n),u^y(t_n),P_k(t_n)\}}{\text{minimize}} \quad \omega_C E_C+\omega_M E_M \tag{8}$$

$$\text{s.t.}\quad P_k(t_n)\leq P_{\max}, \tag{8a}$$

$$\sum_{n=1}^{N}\bar{R}(t_n)\tau\geq B_k,\ \ k=1,\ldots,K, \tag{8b}$$

$$\|\mathbf{u}(t_{n+1})-\mathbf{u}(t_n)\|_2^2\leq(v\tau)^2,\ \ n=1,\ldots,N. \tag{8c}$$

Constraint (8a) sets the maximum MTCD transmit power, and constraint (8b) characterizes the data collection task for each MTCD. Denote by v the maximum flying speed of the UAV, the maximum flying distance of the UAV within a time duration τ is $v\tau$. Thus (8c) can be interpreted as the UAV mobility constraint. Note that the start and end points of the UAV's flight trajectory $\mathbf{u}_s$ and $\mathbf{u}_e$ correspond to the UAV positions at time instants t_1 and t_{N+1}, respectively. In problem $\mathbf{P0}$, the constraints (8a) and (8c) are linear and quadratic constraints. It is straightforward to show that (8a) and (8c) are convex constraints [33]. Therefore, the key to finding the optimal solution to $\mathbf{P0}$, i.e. achieving Global Trajectory Optimization (GTO), lies in whether the objective function and constraints (8b) are convex.

The condition for finding the optimal solution to $\mathbf{P0}$ is stated in the following.

Lemma 1: Define $r_{\max}$ as the UAV station's maximum service radius for data collection, i.e.,

$$r_{\max}=\max\left\{\sqrt{(u^x(t_n)-q_k^x)^2+(u^y(t_n)-q_k^y)^2}\right\},\quad \forall k=1,\ldots,K;\ n=1,\ldots N.$$

There exists a global optimal trajectory for problem $\mathbf{P0}$ if the flying altitude of the UAV satisfies $h_a\geq\sqrt{3}r_{\max}$. ■

The proof of Lemma 1 is presented in the Appendix.

It is worth noting that $h_a\geq\sqrt{3}r_{\max}$ indicates the elevation angle is greater than 60 degrees. According to [32], the probability of LoS propagation is almost 1 when the elevation angle is greater than 60 degrees, even in an urban environment. In this case, the air-to-ground links can be viewed as LoS links and the optimal solution of $\mathbf{P0}$ gives the global optimal trajectory.

III. AEM Modeling and Problem Reformulation

In Section II, we have investigated single-UAV trajectory optimization for energy minimization in an MTCD data collection system. However, as stated in Lemma 1, existence of a global optimal solution to $\mathbf{P0}$ has stringent requirement on the UAV's flying altitude. Specifically, when the ground MTCDs are scattered over a large area, the UAV needs to fly at a very high altitude to guarantee theoretical global optimal solution to $\mathbf{P0}$. This leads to high propagation path-loss of the MTCD-UAV links. Consequently, high communication energy consumption is expected for the data collection tasks, which is undesirable from the energy efficiency perspective.

An intuitive way to mitigate the above issue is to reduce the UAV's flying height so that the LoS link distance between the UAV and the MTCDs is reduced. As a result, the UAV's service radius is reduced as well. It is then reasonable to serve the mMTC network in a clustered manner, where each cluster has a relatively small radius. The UAV station travels across the clusters and collects data from each cluster while hovering above it. The problem then breaks down to the MTCD clustering sub-problem and the in-cluster and inter-cluster UAV flying strategy sub-problems. In this section, we study a modeling technique named artificial energy map (AEM) for analysis of data collection service in the mMTC network. The GLC-AEM scheme, which adopts the divide-and-conquer strategy, is proposed to decouple and solve the EE optimization problem.

Authorized licensed use limited to: UNIVERSITY OF VICTORIA. Downloaded on January 26,2023 at 04:32:29 UTC from IEEE Xplore. Restrictions apply.

A. Constructing the AEM

The radio map is an emerging channel modeling method in UAV communications. It solves the problem that either deterministic or statistical channel model can accurately describe shadow fading. The essence of the radio map is to measure and establish the relationship between the channel state information (CSI) and the geographic location through the cooperation of nodes in the system and establish a database, that is, the radio map. Optimizing UAV communication strategies based on radio map information has become increasingly popular [30], [31]. The radio map can be used to describe exact radio propagation information in UAV communications. In practice, UAVs or other cooperative nodes can establish the relationship between the channel state information (CSI) and the geographic positions of nodes *a priori* by means of spectrum sensing, machine learning etc. A radio map can be constructed and updated after collecting and processing sufficient measurements from the radio propagation environment. Similarly, in this paper, the proposed artificial energy map model studies the relationship between the UAV's data collection energy consumption and the geographical positions of the MTCDs. Based on the position and task information (PTI) of the ground-based MTCDs, we construct an artificial energy function and then generate an AEM that is used to optimize deployment of the UAV station.

Specifically, for a group of MTCDs that are served by a UAV station, we first construct a location-aware energy function according to all MTCDs' PTI. Based on the values of the energy function, a clustering strategy is devised to partition the MTCD set $\mathcal{K}$ into a set of L subsets, i.e. clusters. We use $\mathcal{K}_l$, with $l = 1, \ldots, L$, to denote the l^{th} MTCD cluster. The number of MTCDs in $\mathcal{K}_l$ is K_l, and $\sum_{l=1}^{L} K_l = K$. For the convenience of the notation, we also define a dummy variable $K_0 = 0$. Therefore, the MTCD index subset $\mathcal{K}_l = \{\sum_{i=0}^{i=l-1} K_i + 1, \ldots, \sum_{i=0}^{i=l} K_i\}$. The UAV flies along a trajectory from the preset starting point $\mathbf{u}_s$ to the preset ending point $\mathbf{u}_e$. The trajectory must traverse all clusters, and the UAV collects data from MTCDs within a cluster while hovering above it. The UAV's hovering time in cluster l is denoted as Γ_l, and it uses Δ_l of time to fly from the l^{th} hovering position to the $(l+1)^{\text{th}}$ hovering position. Because the flying attitude of the UAV has a great impact on data transmission, no data transmission from the MTCDs to the UAV is allowed while the UAV is flying between hovering points. The in-cluster hovering time set and the inter-cluster flying time set are denoted by $\mathbf{\Gamma} = \{\Gamma_l\}$ and $\mathbf{\Delta} = \{\Delta_l\}$, respectively. The altitude of the ground is 0, and the flying altitude of the UAV is $h_a(l)$ when it flies over the l^{th} cluster. The coordinates of the ground MTCDs and the UAV's hovering position corresponding to the l^{th} cluster are then expressed as $\mathbf{q}_{k_l} = (q_{k_l}^x, q_{k_l}^y, 0)$ with $k_l \in \mathcal{K}_l$, and $\mathbf{u}(l) = (u^x(l), u^y(l), h_a(l))$, respectively. Similar to eqn. (7), the instantaneous achievable rate from the k_l^{th} MTCD to the UAV station is

$$\bar{R}_{k_l}(\mathbf{u}(l)) = B\log_2\left(1+\frac{P_{k_l}(\mathbf{u}(l))\left(\Pr_{\mathrm{L}}(\mathbf{u}(l))+(1-\Pr_{\mathrm{L}}(\mathbf{u}(l)))\kappa\right)}{\beta_0\sigma^2\|\mathbf{q}_{k_l}-\mathbf{u}(l)\|_2^2}\right) \tag{9}$$

where $P_{k_l}(\mathbf{u}(l))$ is the instantaneous transmit power of the k_l^{th} MTCD in the l^{th} cluster, and $\Pr_{\mathrm{L}}(\mathbf{u}(l))$ is the LoS occurrence probability when the UAV's hovering position is $\mathbf{u}(l)$.

Assume that the amount of data to be transmitted from the k_l^{th} MTCD to the UAV station at the l^{th} hovering position is

$$B_k^l = \Gamma_l \bar{R}_{k_l}(\mathbf{u}(l)),\ k_l \in \mathcal{K}_l, \tag{10}$$

Combining (10) and (9), the communication power consumption of the k_l^{th} MTCD in the l^{th} cluster is derived as

$$P_{k_l}(\mathbf{u}(l)) = \left(2^{\frac{B_k^l}{\Gamma_l}} - 1\right)\frac{\sigma^2}{\bar{h}_{k_l}(\mathbf{u}(l))}, \tag{11}$$

where $\bar{h}_{k_l}(\mathbf{u}(l)) = \frac{(\Pr_{\mathrm{L}}(\mathbf{u}(l))+(1-\Pr_{\mathrm{L}}(\mathbf{u}(l)))\kappa)}{\beta_0\|\mathbf{q}_{k_l}-\mathbf{u}(l)\|_2^2}$.

We define a communication power matrix and use it to establish the relationship between the MTCD clustering strategy and the communication energy consumption, which is given as

$$\mathbf{Q}_k = \begin{bmatrix} P_1(\mathbf{u}(1)) & P_1(\mathbf{u}(2)) & \cdots & P_1(\mathbf{u}(L)) \\ P_2(\mathbf{u}(1)) & P_2(\mathbf{u}(2)) & \cdots & P_2(\mathbf{u}(L)) \\ \vdots & \vdots & \ddots & \vdots \\ P_K(\mathbf{u}(1)) & P_K(\mathbf{u}(2)) & \cdots & P_K(\mathbf{u}(L)) \end{bmatrix}. \tag{12}$$

The number of non-zero entries in the k^{th} column of $\mathbf{Q}_k$ is therefore K_l. Considering the fact that the number of ground-to-air links a UAV station can support is limited, an upper bound on K_l is introduced, i.e. $K_l \le S_{\max}$. The energy function for clustering is defined as

$$\mathcal{E}_k(\mathbf{u}(l)) = \left(2^{\frac{B_k}{\Gamma_l}} - 1\right)\frac{\sigma^2}{h_k(\mathbf{u}(l))}\Gamma_l,\ k = 1, \ldots, K. \tag{13}$$

Eqns. (12) and (13) are used to determine the clustering strategy, which will be further discussed in detail in Section IV. Note that when determining the clustering scheme, $\mathbf{u}(l)$'s are updated as the positions of the cluster heads.

After determining the clustering scheme, the in-cluster UAV hovering positions for data collection should be optimized. The following artificial energy function (AEF) is constructed, and an AEM is generated accordingly for each cluster.

$$\Phi_l = \sum_{k_l\in\mathcal{K}_l} P_{k_l}(\mathbf{u}(l))\Gamma_l - \sum_{k_l\in\mathcal{K}_l}\log\left(P_{\max} - P_{k_l}(\mathbf{u}(l))\right) + P_h\Gamma_l. \tag{14}$$

In (14), P_{k_l} is the transmit power of the k_l^{th} MTCD in this cluster, and $P_h = \sqrt{\frac{(m_v g)^3}{2\pi\rho r_{\mathrm{p}}^2 n_{\mathrm{p}}}}$ is the hovering power. The lowest AEM point corresponds to the energy-efficient optimal UAV hovering position in the cluster. Taking the negative gradient of the AEF (14) as the gravitational function φ_l, we have

$$\begin{aligned}\varphi_l &= -\nabla\Phi_l \\ &= -\sum_{k_l\in\mathcal{K}_l}\left(\frac{\partial P_{k_l}(\mathbf{u}(l))}{\partial u^x(l)} + \frac{\partial P_{k_l}(\mathbf{u}(l))}{\partial u^y(l)} + \frac{\partial P_{k_l}(\mathbf{u}(l))}{\partial \Gamma_l}\right) \\ &\quad \left(\Gamma_l + \frac{1}{P_{\max} - P_{k_l}(\mathbf{u}(l))}\right) - \sum_{k_l\in\mathcal{K}_l} P_{k_l}(\mathbf{u}(l)) - P_h.\end{aligned} \tag{15}$$

Authorized licensed use limited to: UNIVERSITY OF VICTORIA. Downloaded on January 26,2023 at 04:32:29 UTC from IEEE Xplore. Restrictions apply.

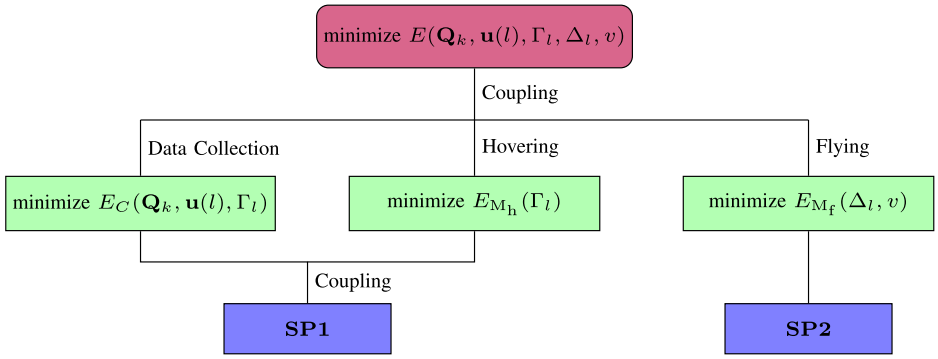

Fig. 2. Decomposition of the optimization problem.

The UAV adjusts its position under the action of the gravitational function. Finally, based on the above principle, the UAV arrives at the lowest point of the AEM and claims it the EE optimal hovering position for data collection in the current cluster.

B. Problem Reformulation With AEM

Assume that the power consumption of the UAV receiver is a constant circuit power, which does not affect the optimization process. The overall communication energy consumption for data transmission is thus given by

$$E_C(\mathbf{Q}_k, \mathbf{u}(l), \Gamma_l) = \sum_{l=1}^{L} \sum_{k_l \in \mathcal{K}_l} P_{k_l}(\mathbf{u}(l))\Gamma_l. \tag{16}$$

There are two maneuvering states of the UAV, hovering and flying, in the reformulated model. As in [29], the UAVs' maneuvering energy consumption is the sum of hovering energy consumption and flying energy consumption

$$E_{\mathrm{M}}(\Gamma_l, \Delta_l, v) = E_{\mathrm{M_f}}(\Delta_l, v) + E_{\mathrm{M_h}}(\Gamma_l),\ l = 1, \ldots, L, \tag{17}$$

where $E_{\mathrm{M_f}}$ and $E_{\mathrm{M_h}}$ are flying and hovering energies given by

$$E_{\mathrm{M_f}}(\Delta_l, v) = \sum_{l=1}^{L} \frac{m_{\mathrm{v}} g}{\eta_{\mathrm{m}} \eta_{\mathrm{p}}} v \Delta_l, \tag{18}$$

$$E_{\mathrm{M_h}}(\Gamma_l) = \sum_{l=1}^{L} \sqrt{\frac{(m_{\mathrm{v}} g)^3}{2\pi\rho r_{\mathrm{p}}^2 n_{\mathrm{p}} \eta_{\mathrm{m}}^2 \eta_{\mathrm{p}}^2}} \Gamma_l. \tag{19}$$

In (19), r_{p} and n_{p} denote the radius and the number of the UAV's propellers. The total energy consumption of the mMTC data collection system is given by the sum of the communication energy and the UAV maneuvering energy.

$$E(\mathbf{Q}_k, \mathbf{u}(l), \Gamma_l, \Delta_l, v) = \omega_C E_C(\mathbf{Q}_k, \mathbf{u}(l), \Gamma_l) + \omega_M E_{\mathrm{M}}(\Gamma_l, \Delta_l, v) \tag{20}$$

The original problem is reformulated as

$$\mathbf{P1}: \underset{\{\mathbf{Q}_k, \mathbf{u}(l), \Gamma_l, \Delta_l, v\}}{\text{minimize}} \quad E(\mathbf{Q}_k, \mathbf{u}(l), \Gamma_l, \Delta_l, v) \tag{21}$$

$$\text{s.t.} \quad P_k(\mathbf{u}(l)) \le P_{\max}, \tag{21a}$$

$$S_{\min} \le K_l \le S_{\max}, \tag{21b}$$

$$\sum_{l=1}^{L} K_l = K. \tag{21c}$$

Constraint (21a) is the per-MTCD transmit power constraint. The inequality (21b) sets a reasonable range for the cluster size, i.e. the number of MTCDs a UAV station serves simultaneously. The last constraint (21c) ensures that every MTCD is served. It can be observed from the system model that the structure of the communication power consumption matrix $\mathbf{Q}_k$, the UAV hovering position and hovering time in each cluster, the UAV's inter-cluster flying time, as well as the maximum flying speed all have impacts on the overall energy consumption. It is challenging to jointly optimize all these variables analytically to achieve total energy consumption minimization.

IV. The Proposed AEM-Based UAV Trajectory Planning Method

To solve problem $\mathbf{P1}$ given by (21), we propose to decouple the clustering, hovering and flying variables such that the original problem is decomposed into sub-problems that are tractable. The optimization objective is to minimize the total energy consumption. The communication energy consumption, as discussed above, is affected by the clustering strategy and the UAV's hovering strategy. Once the optimal hovering strategy is obtained, the hovering energy minimization problem is solved. On the other hand, the factors affecting the UAV's flying energy consumption in (18) include the UAV speed and the flying time. Minimizing the UAV flying energy is equivalent to minimizing the trajectory length. Therefore, once the hovering strategy is determined, the UAV flying strategy design is essentially a classic salesman problem that is readily solved by techniques such as Ant Colony Optimization (ACO). To make this difficult coupling problem solvable, we do not consider the impact of the UAV flying strategy on the clustering and hovering strategies. The problem decomposition process is shown in Fig. 2.

Sub-problem $\mathbf{SP1}$ jointly optimizes the MTCD clustering strategy and the UAV hovering strategy. An iterative alternating optimization procedure can be employed to solve $\mathbf{SP1}$. After obtaining the MTCD clustering and UAV hovering schemes, sub-problem $\mathbf{SP2}$ minimizes the UAV flying energy consumption through finding the optimal inter-cluster flying path. Next,

Authorized licensed use limited to: UNIVERSITY OF VICTORIA. Downloaded on January 26,2023 at 04:32:29 UTC from IEEE Xplore. Restrictions apply.

we are going to present the detailed solution based on the above decomposition approach.

A. GLC-AEM Algorithm for Clustering and UAV Hovering Strategy Design

The joint optimization sub-problem **SP1** for MTCD clustering and the UAV hovering strategy design is given in the following.

$$\mathbf{SP1}: \underset{\{\mathbf{Q}_k,\mathbf{u}(l),\Gamma_l\}}{\text{minimize}} \quad \omega_C E_C(\mathbf{Q}_k,\mathbf{u}(l),\Gamma_l)+\omega_M E_{\mathrm{M_h}}(\Gamma_l) \tag{22}$$

$$\text{s.t.} \quad P_k(\mathbf{u}(l)) \le P_{\max}, \tag{22a}$$

$$S_{\min} \le K_l \le S_{\max}, \tag{22b}$$

$$\sum_{l=1}^{L} K_l = K. \tag{22c}$$

Problem **SP1** is a non-convex optimization problem. The optimization variables $\mathbf{Q}_k$, Γ_l and $\mathbf{u}(l)$ are still coupled in the objective function (22). The MTCD clustering strategy and the UAV hovering strategy therefore interact with each other in **SP1**. To tackle this, a greedy learning approach based on the AEM model can be used to effectively group the MTCDs from the EE perspective, while the optimal UAV hovering strategy within one cluster can be obtained by applying the AEM principle. We therefore propose an iterative alternating optimization method, namely the GLC-AEM algorithm, for problem **SP1**.

1) The Greedy Learning Clustering (GLC) Algorithm: A convenient yet efficient strategy based on the K-means principle is employed for MTCD clustering. First, the distance between adjacent MTCDs is analyzed according to the MTCDs' spatial distribution. The number of clusters is then determined based on the MTCD distribution density and the UAV's service parameters. Specifically, the probability of exactly α MTCDs in an area is given by

$$\Pr(x=\alpha)=\frac{\lambda^{\alpha}}{\alpha!}e^{-\lambda}. \tag{23}$$

Assume the MTCDs are uniformly distributed within a circle of radius r with density ρ. The expected number of MTCDs in this area is $\lambda=\rho\pi r^2$. Therefore,

$$\Pr(x=\alpha)=\frac{(\rho\pi r^2)^{\alpha}}{\alpha!}e^{-\rho\pi r^2}. \tag{24}$$

The probability of at least one MTCD in this area is

$$\Pr(\alpha\ge 1)=1-\Pr(x=0)=1-e^{-\rho\pi r^2}. \tag{25}$$

Denote by d_{adj} the distance between adjacent MTCDs. It is straightforward to show that

$$\Pr(d_{\mathrm{adj}}\le r)=\Pr(\alpha\ge 1)=1-e^{-\rho\pi r^2}\doteq F(r). \tag{26}$$

The probability density function of the inter-MTCD distance is

$$f_R(r)=F'(r)=2\pi\rho r e^{-\rho\pi r^2}. \tag{27}$$

Algorithm 1: Clustering Number Determining (CND) Algorithm.

Input: The MTCD set $\mathcal{K}$, maximum and minimum cluster size $S_{\max}$ and $S_{\min}$, the MTCDs' distribution density ρ.

Output: The optimal number of MTCD clusters, L_{opt}.

1: Initialization: Initialize clustering number as $L_{\mathrm{ini}}=1$.
Repeat
2: Divide the MTCDs into L_{ini} clusters using the K-means clustering algorithm with $k=L_{\mathrm{ini}}$.
3: Calculate the maximum cluster radius $r_{\max}$ according to the clustering result and count the number of MTCDs K_l in each cluster.
4: **if** $r_{\max}\le\sqrt{\frac{S_{\max}}{\rho\pi}}$ and $S_{\min}\le K_l\le S_{\max}$ **then**
5: $L_{\mathrm{opt}}=L_{\mathrm{ini}}$
6: **else**
7: $L_{\mathrm{ini}}=L_{\mathrm{ini}}+1$
8: **end if**
9: Iterate this process to the preset number and choose a L_{opt} and initial clustering strategy under principle CP-I or CP-II.

The expectation of r is therefore

$$\begin{aligned}\mathbb{E}[r]&=\int_0^{+\infty} r f_R(r)dr=\int_0^{+\infty}2\pi\rho r^2 e^{-\rho\pi r^2}dr\\&=\int_0^{+\infty}e^{-\rho\pi r^2}dr=\frac{1}{2\sqrt{\rho}}.\end{aligned} \tag{28}$$

It can be observed that the distance between adjacent MTCDs is related to the distribution density of the MTCDs. When the MTCDs' density grows large, the distance between adjacent MTCDs approaches 0, which is intuitively correct. Therefore, when clustering the MTCDs in an mMTC network, the number of clusters should be determined according to the MTCD distribution density and the number of MTCDs that the UAV can serve at the same time.

We investigate two principles for the Clustering Number Determining (CND) algorithm, which determines the optimal number of clusters before the MTCDs are grouped into clusters. To collect delay-sensitive data, it is desirable to serve as many MTCDs simultaneously as possible from the delay perspective, subject to certain constraints. Correspondingly, the Clustering Principle I (CP-I) is to minimize the number of clusters under the constraints of the UAV's service radius and service capacity. The UAV station flies to the optimal hovering position of each cluster to collect the delay-sensitive data. Conversely, for delay-insensitive data, the Clustering Principle II (CP-II) tries to minimize the communication energy consumption as much as possible. The CP-II principle of CND therefore aims to minimize the maximum clustering radius $r_{\max}$ so that the energy consumption for data transmission is minimized. The CND procedure is summarized in Algorithm 1.

Authorized licensed use limited to: UNIVERSITY OF VICTORIA. Downloaded on January 26,2023 at 04:32:29 UTC from IEEE Xplore. Restrictions apply.

Algorithm 2: Greedy Learning Clustering (GLC) Algorithm.

Input: The MTCD set $\mathcal{K}$, data collection tasks B_k, the channel coefficients $h_k(t_n)$, maximum and minimum cluster size $S_{\max}$ and $S_{\min}$, AWGN power σ^2, hovering time set $\mathbf{\Gamma}$.

Output: The optimal $\mathbf{Q}_k^*$.

1: Initialization: Clustering obtained by applying Algorithm 1 is used as the initial clustering $\mathcal{L}$. Calculate $\mathbf{Q}_k$ based on $\mathcal{L}$.
2: Count the number of non-zero entries in each column of $\mathbf{Q}_k$ as $K_l, \forall l \in \mathcal{L}$. **Repeat**
3: **for** every MTCD $k \in \mathcal{K}$ **do**
4: The current cluster of the k^{th} MTCD is recorded as l_c.
5: **for** every cluster $l \in \mathcal{L}$ **do**
6: Generate the energy function of the k^{th} MTCD as $\mathcal{E}_k(\mathbf{u}(l)) = (2^{\frac{B_k}{\Gamma_l}} - 1)\frac{\sigma^2}{h_k(\mathbf{u}(l))}\Gamma_l$, and the set $\vartheta(l) \triangleq \{\mathcal{E}_k(\mathbf{u}(l)), l \in \mathcal{L}\}$.
7: **end for**
8: **while** $\min\{\vartheta(l)\} < P_k(\mathbf{u}(l_c))$ **do**
9: $l_o = \arg\min\ \vartheta(l)$,
10: **if** $K_{l_o} > S_{\max}$ or $K_{l_c} < S_{\min}$ **then**
11: $\mathcal{E}_k(\mathbf{u}(l_c)) = +\infty$
12: **else**
13: Modify the cluster index of MTCD k from l_c to l_o and update $\mathbf{Q}_k$; $K_{l_o} = K_{l_o} + 1,\ K_{l_c} = K_{l_c} - 1$.
14: **end if**
15: **while**
16: **endfor**
17: **Until** the value of $\mathbf{Q}_k$ does not change or a preset maximum number of iterations is reached.

After obtaining an initial clustering scheme based on the K-means principle, a Greedy Learning Clustering (GLC) algorithm based on the AEM principle is proposed to iteratively update the clusters. Specifically, an energy function based on the initial cluster heads and the PTI of the MTCDs is constructed as the lost function. Next, clustering of the MTCDs is updated by learning the energy function. Then the MTCDs generate the AEM to conduct AEM-based hovering position optimization, as will be studied in the next part. In the next iteration of the GLC algorithm, each cluster head is adjusted to the optimal in-cluster UAV hovering position obtained in the last iteration. The above process is iterated until convergence, and the optimal clustering and UAV hovering strategies are output by the algorithm. Algorithm 2 shows detailed steps of how the MTCDs learn the energy function and adjust clustering iteratively.

2) AEM-Based Optimal UAV Hovering Strategy Design: The in-cluster hovering position of the UAV can be optimized given MTCDs in the mMTC network are clustered. Specifically, we first generate an AEM according to (14) for every cluster. As summarized in Algorithm 3, the UAV adjusts its position under the action of the gravitational function. The UAV finally arrives at the lowest point of the AEM under the action of the combined gravitational function and claims it the optimal hovering position. At this hovering position, the energy consumption is the lowest for the cluster, as shown in Fig. 5.

TABLE II
PARAMETER VALUES OF THE SYSTEM SETTING FOR SIMULATIONS

v	$20\,m/s$	σ^2	-174 dBm/Hz	B	10 kHz
m	$0.5\,kg$	r_p	$30\,cm$	r_p	$30\,cm$
n_p	4	η_m	0.94	η_p	0.85
a	9.6	β_0	45 dB	κ	0.2
b	0.28	T	$50\,s$	N	100
ω_C	1	ω_M	1	-	-

Algorithm 3: UAV Hovering Strategy Optimization Based on AEM Modeling.

Input: Positions of all MTCDs in cluster l, data collection tasks B_k^l, UAV's flying altitude $h_a(l)$, and AWGN power σ^2.

Output: Optimal UAV hovering scheme, i.e., optimal hovering position $\mathbf{u}^*(l)$ and optimal hovering time Γ_l^*, for the l^{th} cluster.

1: Initialization: The cluster head in Algorithm 2 is used as the initial hovering position $\mathbf{u}(l)$. The hovering time $\Gamma_l = \max\{\frac{B_k^l}{R_{k_l}(\mathbf{u}(l))}\}$.
2: **Repeat**
3: Calculate the transmit power of the k_l^{th} MTCD as $P_{k_l}(\mathbf{u}(l)) = (2^{\frac{B_k^l}{\Gamma_l}} - 1)\frac{\sigma^2}{h_{k_l}(\mathbf{u}(l))}$;
4: Calculate the The AEF function and generate the AEM, the AEF function is $\Phi_l = \sum_{k_l \in \mathcal{K}_l} P_{k_l}(\mathbf{u}(l))\Gamma_l - \sum_{k_l \in \mathcal{K}_l} \log(P_{\max} - P_{k_l}(\mathbf{u}(l))) + P_h\Gamma_l$.
5: Calculate the combined gravitational function as $\varphi_l = -\nabla\Phi_l\mathbf{e}$.
6: The UAV adjusts the hovering strategy under the action of the combined gravitational function. Update $\mathbf{u}(l)$ and Γ_l.
7: **Until** terminate at convergence or a preset maximum number of iterations is reached.

Problem $\mathbf{SP1}$ can be solved by alternately optimizing the clustering strategy using the GLC algorithm and the UAV hovering strategy using the AEM-based algorithm. It is worth noting that in the iterative process, the cluster head in Algorithm 2 is adaptively adjusted with the optimal hovering position of the UAV in Algorithm 3. The data collection energy consumption and the UAV hovering energy consumption decrease as the GLC-AEM algorithm iterates until convergence.

B. Inter-Cluster UAV Flying Trajectory Planning

To achieve the overall optimization objective of problem $\mathbf{P1}$, we next optimize the UAV's inter-cluster flying trajectory. The corresponding sub-problem, according to Fig. 2, is given as

$$\mathbf{SP2}:\ \text{minimize}\quad E_{\text{M}_\text{f}}(\Delta_l, v) \tag{29}$$

Authorized licensed use limited to: UNIVERSITY OF VICTORIA. Downloaded on January 26,2023 at 04:32:29 UTC from IEEE Xplore. Restrictions apply.

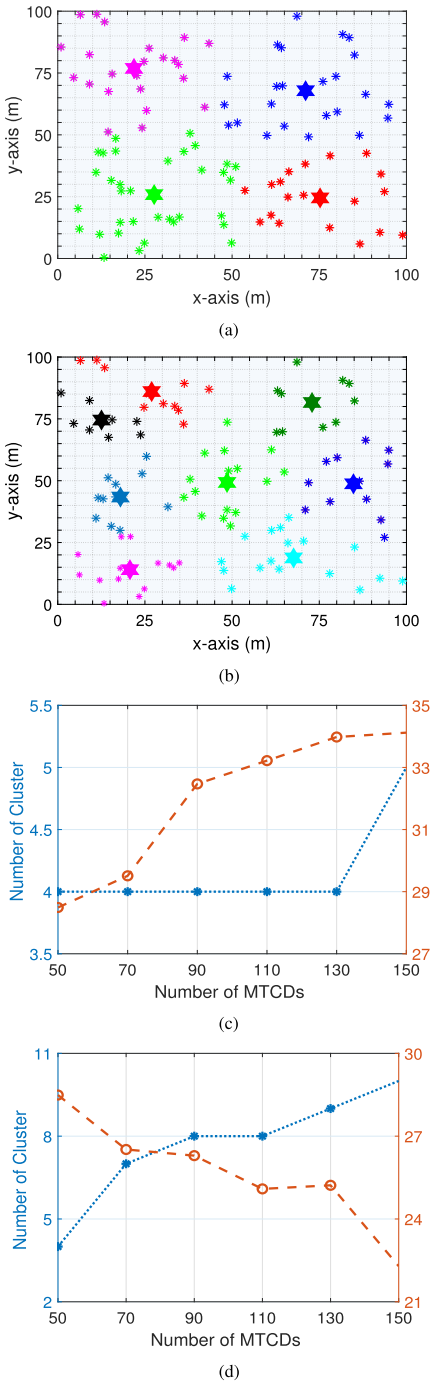

Fig. 3. Optimized clustering results by the CND algorithm under different principles, with 100 uniformly distributed MTCDs. (a) Clustering results under the principle of minimizing the cluster numbers (CP-I). (b) Clustering results under the principle of minimizing $r_{\max}$ (CP-II). (c) Average L_{opt} and $rfig2a_{\max}$ under the principle of minimizing the cluster numbers (CP-I). (d) Average L_{opt} and $r_{\max}$ under the principle of minimizing $r_{\max}$ (CP-II).

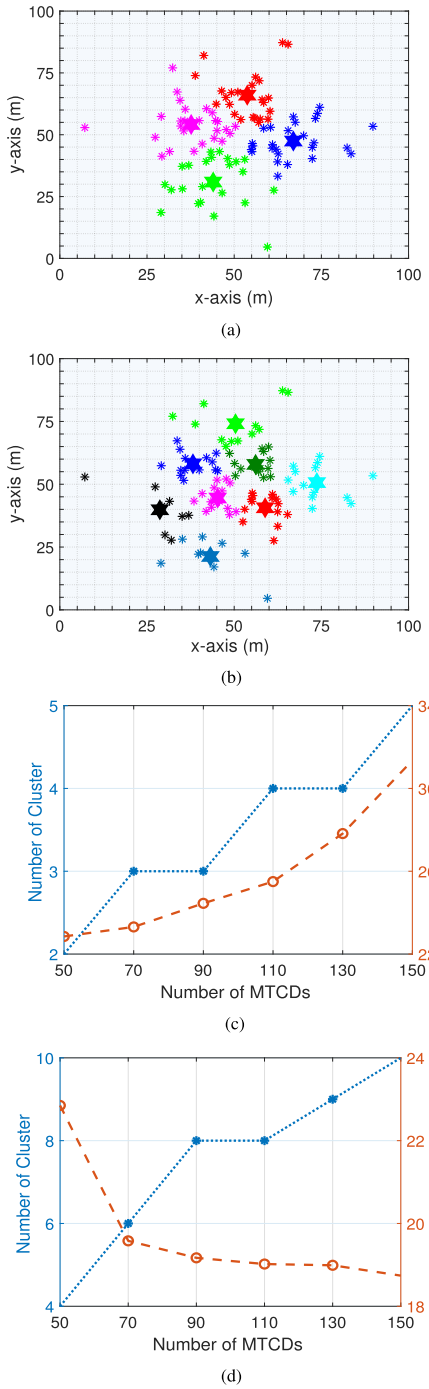

Fig. 4. Optimized clustering results by the CND algorithm under different principles, with 100 Gaussian distributed MTCDs. (a) Clustering results under the principle of minimizing the cluster numbers (CP-I). (b) Clustering results under the principle of minimizing $r_{\max}$ (CP-II). (c) Average L_{opt} and $r_{\max}$ under the principle of minimizing the cluster numbers (CP-I). (d) Average L_{opt} and $r_{\max}$ under the principle of minimizing $r_{\max}$ (CP-II).

As mentioned at the beginning of this section, the impact of the UAV flying strategy on the clustering and hovering strategies is ignored. The UAV's inter-cluster flying energy consumption therefore only depends on the UAV's speed and flying time. Sub-problem **SP2** can be equivalently transformed into a traveling distance minimization problem, which is readily solved by algorithms, e.g. ACO algorithm, for the traveling salesman problem.

C. Extension to the Multi-UAV Scenario

It is worth noting that the proposed GLC-AEM algorithm can be extended to multi-UAV application scenarios to overcome

Authorized licensed use limited to: UNIVERSITY OF VICTORIA. Downloaded on January 26,2023 at 04:32:29 UTC from IEEE Xplore. Restrictions apply.

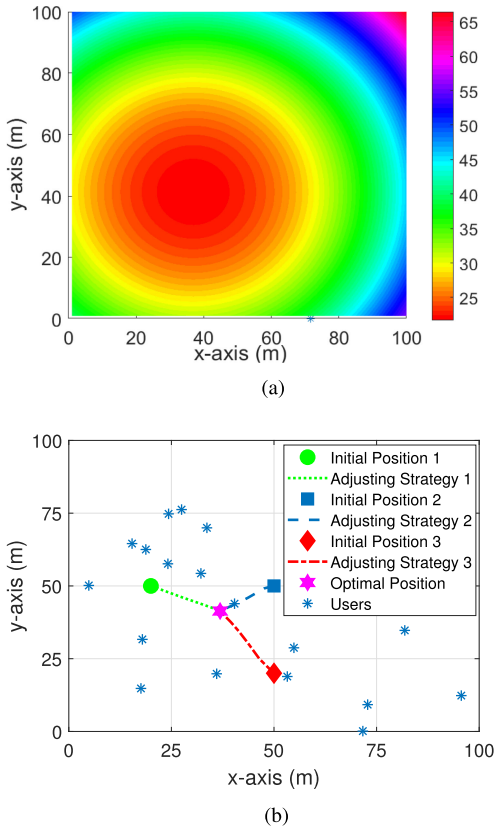

Fig. 5. Demonstration of the AEM model and the AEM-based optimal UAV hovering strategy. (a) An Artificial Energy Map. (b) Optimal hovering strategy obtained by convex optimization.

the drawback of the single-UAV system, i.e., the long mission time due to the sequential operation. Deploying multiple UAVs for data collection enables parallel operation, which significantly reduces the mission time. In a multi-UAV MTCD data collection system, the clustering and hovering strategies, i.e. Algorithms 1, 2 and 3, are still applicable. After the clustering and the in-cluster hovering strategies are determined, the inter-cluster trajectory optimization deals with a multiple travelling salesmen problem, instead of a single salesman problem in the single-UAV scenario. Specifically, after obtaining all hovering strategies through the GLC-AEM algorithm, the hovering points are clustered again by applying the K-means principle. Each UAV uses the Ant Colony Optimization (ACO) algorithm to obtain a closed-loop trajectory in each cluster consisting of multiple hovering points.

V. Computational Complexity Analysis

The complexity of the algorithms under investigation largely depends on the scale (number of operational parameters) of the problem. For the GTO algorithm in Section II-C, establishing an N-step trajectory involves all the $K \times N$ transmit power variables $P_k(t_n)$, as well as the $2N$ coordinate variables of the trajectory anchor points. The total number of operational variables involved in the GTO problem is therefore $\nu_0 = N(K+2)$. Also, for the GTO algorithm, the number of constraints in the optimization problem, denoted by $\kappa_0 = KN + K + N$, is another important factor. If we a gradient-based method (say, Newton's method) is employed to solve the convex optimization problem, for each step of decent, we have to find the product $\mathbf{H}^{-1}\mathbf{g}$, where $\mathbf{H}$ is the $\nu_0 \times \nu_0$ Hessian matrix, and $\mathbf{g}$ is a $\nu_0 \times 1$ vector. The complexity of this process is $O(\kappa_0 \nu_0^2)$. Furthermore, the number of iterations of Newton steps grows as $\sqrt{\kappa_0}$ [33].

The GLC-AEM algorithm, on the other hand, consists of three parts, the GLC algorithm for MTCD clustering, the AEM-based optimization of the hovering positions, and the ACO algorithm for obtaining the optimal inter-cluster flying path. First, the complexity of GLC clustering is determined by the k-means algorithm, which is given by $O(c_0 K)$, where $c0$ is usually small and determined by the number of clusters, the sample dimension and the number of iterations. Next, evaluation of the complexity of the AEM algorithm is similar to that of the GTO. Here, the number of design variables is simply the coordinates of each hovering point $(u^x(l), u^y(l))$ and the hovering time Γ_l, i.e., $\nu_R = 3$. For each cluster, the GLC-AEM algorithm calculates $(u^x(l), u^y(l))$ and Γ_l by following the AEM principle. Similar in steps to the analysis of the GTO algorithm, we have to find $-\nabla\Phi_l \mathbf{e}$ for adjusting the hovering strategy in each step. The complexity of this step is $O(\nu_{\mathrm{R}})$, which is much lower than that of the GTO algorithm. Finally, the complexity of the ACO algorithm for optimal flying route selection only depends on the number of ants and the iteration times, not on the number of optimization variables or constraints. The complexity of the ACO algorithm is thus not significantly affected by the size of the problem. Therefore, the overall complexity of GLC-AEM is lower than that of the GTO algorithm, and the system's scale has little impact on its complexity.

VI. Simulation Results

In this section, we study through simulations the performance of the proposed GLC-AEM scheme for energy-efficient deployment of UAV-enabled data collection system in clustered mMTC networks. The simulation study consists of three parts. Firstly, the MTCD clustering results based on the CND algorithm are presented under both the CP-I and CP-II principles. In the second place, the GLC-AEM strategy is simulated. Specifically, optimization of the UAV's in-cluster hovering position based on construction of an AEM is demonstrated. The results of both GLC-based and K-means-based clustering are presented. The effect of the GLC-AEM scheme in reducing communication energy consumption and hovering energy consumption is verified by simulations. Finally, the trajectories of the UAV determined by the GTO and the GLC-AEM schemes are presented, and the advantages of the proposed GLC-AEM scheme in improving energy efficiency is discussed. The energy consumption and delay performance of applying the GLC-AEM strategy to multi-UAV scenarios are also investigated through simulations.

System setting parameters and their values used in the simulations are summarized in Table II.

A. Determining the Optimal Number of Clusters

The proposed CND algorithm basically follows one of the following two principles. The first principle CP-I is to minimize the total number of clusters. By doing this, the number of MTCDs

Authorized licensed use limited to: UNIVERSITY OF VICTORIA. Downloaded on January 26,2023 at 04:32:29 UTC from IEEE Xplore. Restrictions apply.

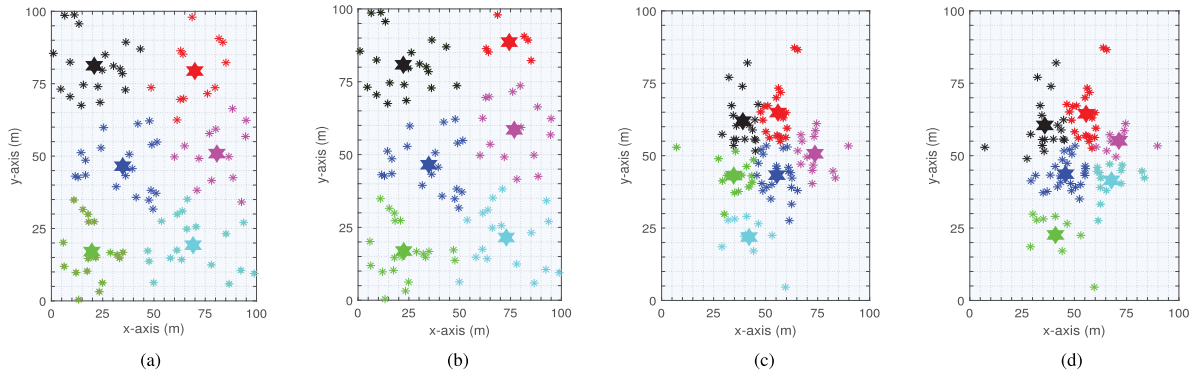

Fig. 6. Comparison of clustering results between the GLC and K-means algorithms. (a) Clustering of 60 uniformly distributed MTCDs by the K-means principle. (b) Clustering of 60 uniformly distributed MTCDs by the GLC algorithm. (c) Clustering of 60 Gaussian distributed MTCDs by the K-means principle. (d) Clustering of 60 Gaussian distributed MTCDs by the GLC algorithm.

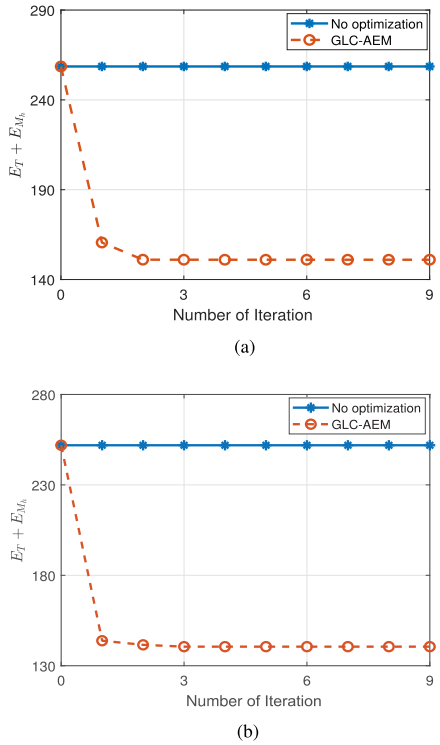

Fig. 7. The communication and hovering energy consumption achieved by the AEM-GLC algorithm through joint optimization of clustering and hovering strategies. (a) Simulation with 60 uniformly distributed MTCDs. (b) Simulation with 60 Gaussian distributed MTCDs.

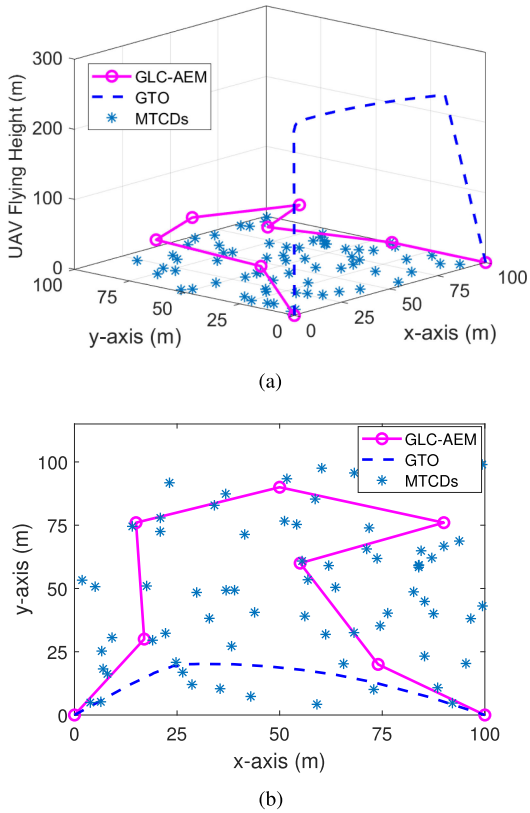

Fig. 8. Comparison of the trajectories given by the GTO and GLC-AEM algorithms, with 60 uniformly distributed MTCDs. (a) 3D trajectories given by the GTO and GLC-AEM algorithms. (b) 2D horizontal trajectories given by the GTO and GLCAEM algorithms.

served by the UAV station simultaneously is made as large as possible, which is desirable for delay-sensitive applications. While for collection of delay-insensitive data, the focus is more on reducing the communication energy consumption. By employing the CP-II principle, the CND algorithm minimizes $r_{\max}$ so that the link distance is made as small as possible, which in turn minimizes the communication power. The clustering results are shown in Figs. 3 and 4. The minimum and maximum cluster sizes are $S_{\min} = 5$ and $S_{\max} = 40$. A total of 100 MTCDs are uniformly distributed over a 100 m $\times$ 100 m geographic area in Fig. 3, and the 100 MTCDs are distributed following a truncated Gaussian distribution in Fig. 4.

As shown in Figs. 3 and 4, when the CP-I principle is adopted, the number of clusters is small and $r_{\max}$ is large. As expected, this principle tends to form large clusters to reduce the time spent on data collection. The number of clusters L_{opt} and the cluster radius $r_{\max}$ increase with the number of MTCDs. When the CP-II principle of minimizing $r_{\max}$ is adopted, the number of clusters is larger, and $r_{\max}$ is smaller, compared to the results

Authorized licensed use limited to: UNIVERSITY OF VICTORIA. Downloaded on January 26,2023 at 04:32:29 UTC from IEEE Xplore. Restrictions apply.

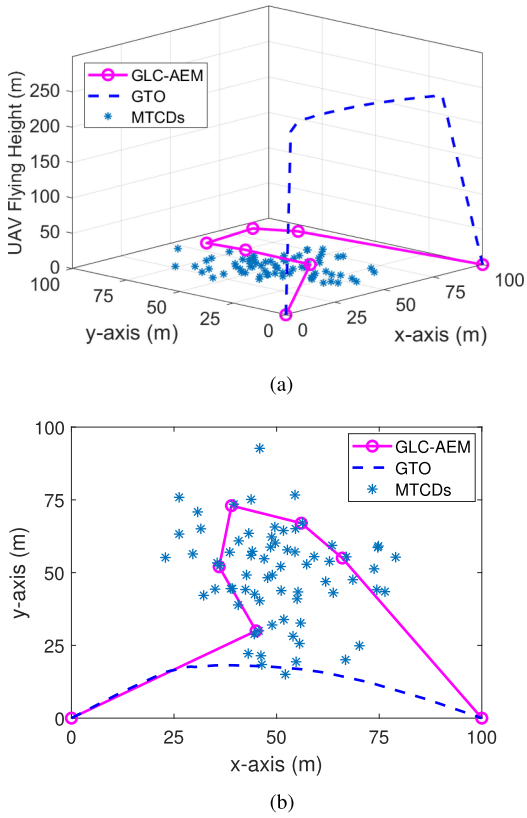

Fig. 9. Comparison of the simulated trajectories given by the GTO and GLC-AEM algorithms, with 60 Gaussian distributed MTCDs. (a) 3D trajectories given by the GTO and GLC-AEM algorithms. (b) 2D horizontal trajectories given by the GTO and GLCAEM algorithms.

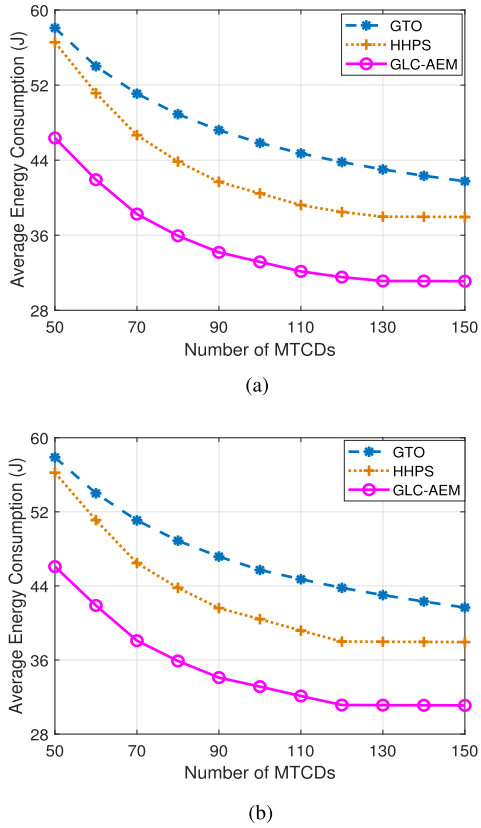

Fig. 10. The average energy consumption per MTCD. (a) Simulation with 60 uniformly distributed MTCDs. (b) Simulation with 60 Gaussian distributed MTCDs.

with CP-I. As the number of MTCDs increases, the number of clusters also increases, while $r_{\max}$ decreases.

B. Performance Evaluation of the GLC-AEM Algorithm

1) The AEM Model: We next demonstrate the proposed AEM modelling technique. In the simulation, 20 MTCDs are uniformly distributed in a 100 m $\times$ 100 m geographical area. Randomly generated tasks following uniform distribution $B_k \sim U(0, 2.4)$ Mb are assigned to the MTCDs. There are three initial horizontal hovering positions $[20, 50]$, $[50, 20]$ and $[50, 50]$. The hovering time is fixed to 10 seconds. The simulation results are shown in Fig. 5.

It can be observed from Fig. 5(a) that a lowest energy point exists in the energy map generated according to the AEF (14). Following the direction of the fastest energy decline in the AEM, we show in Fig. 5(b) the movement of the UAV from the initial hovering positions to the optimal hovering position. It has been observed from the numerical results that the optimal hovering position attained in Fig. 5(b) agrees with the lowest energy point in the AEM, which validates the proposed AEM-based modeling and optimization technique.

2) Greedy Learning Clustering: We next evaluate the GLC algorithm for MTCD clustering. In Fig. 6(a) and (b), 60 MTCDs are uniformly distributed in a 100 m $\times$ 100 m geographical area. Similarly, 60 Gaussian distributed MTCDs are considered in

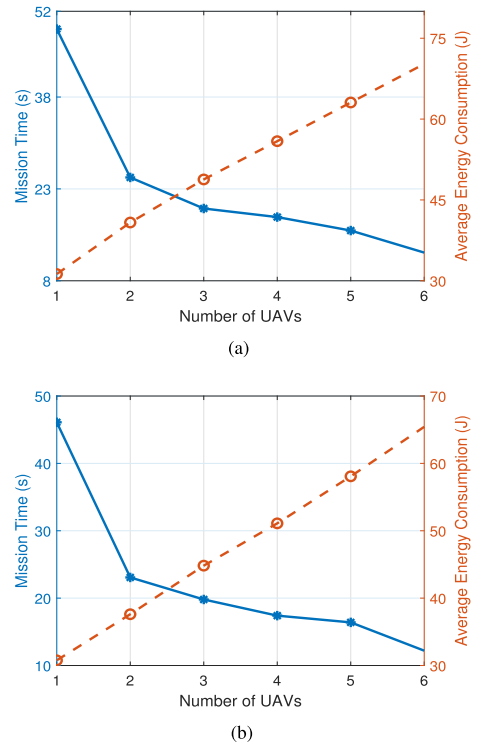

Fig. 11. The average energy consumption and total mission time with different number of UAVs. (a) Simulation with 150 uniformly distributed MTCDs. (b) Simulation with 150 Gaussian distributed MTCDs.

Authorized licensed use limited to: UNIVERSITY OF VICTORIA. Downloaded on January 26,2023 at 04:32:29 UTC from IEEE Xplore. Restrictions apply.

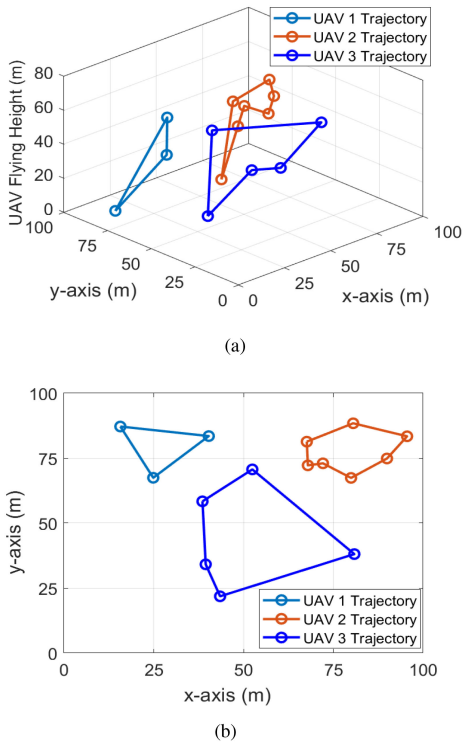

Fig. 12. Demonstration of the optimal UAV 3-D trajectories given by the GLC-AEM algorithms in the multi-UAV scenario, with 200 uniformly distributed MTCDs. (a) 3D trajectories given by the GLC-AEM algorithm. (b) 2D horizontal trajectories given by the GLC-AEM algorithm.

Fig. 6(c) and (d). Let $S_{\min} = 5$, $S_{\max} = 40$ and a set of tasks are randomly generated according to $B_k \sim U(0, 2.4)$ Mb. It is observed that the results for GLC shown in Fig. 6(b) and (d) are very different from that for the K-means algorithm shown in Fig. 6(a) and 6(c). The underlying reason for the phenomenon is that the GLC-AEM clustering strategy is determined by the channel conditions and transmission tasks of each MTCDs, while the initial K-means clustering strategy is solely based on the Euclidean distance. The GLC-AEM scheme better utilizes the factors that have impact on communication energy consumption to better serve the data collection tasks. Its effect on energy reduction will be studied in more detail later.

3) Data Collection Energy Consumption of GLC-AEM: The optimal UAV hovering strategy in each cluster can be determined by employing the AEM principle. And according to the GLC algorithm, the clustering strategy of the mMTC network can be adjusted according to the hovering strategy. Through iteratively alternating the GLC-based clustering and the AEM-based in-cluster hovering optimization processes, the data collection energy consumption and the UAV hovering energy consumption are monotonically decreasing until convergence. The simulation results are shown in Fig. 7. The proposed AEM-GLC algorithm reduced the data collection energy consumption by about 44%, compared with the original scheme based on K-means clustering. This also validates effectiveness of incorporating GLC with the AEM-based UAV hovering strategy optimization from the energy efficiency perspective.

C. UAV Trajectories and Total Energy Consumption

In this part, the optimized UAV trajectories are presented. The total energy consumption achieved by the GLC-AEM strategy is presented, which is compared with that achieved by the GTO optimization method. Both uniformly distributed and Gaussian distributed MTCDs were considered in the simulations.

Firstly, we show the simulated process of the UAV traversing the entire data collection area based on the GLC-AEM algorithm. In the simulation, a set of tasks were randomly generated according to $B_k \sim U(0, 2.4)$ Mb. The clustering and hovering strategies were determined by the CND and GLC-AEM algorithms. The UAV's flying altitude is set to $h_a = \sqrt{3} r_{\max}$. After adjusting the clustering strategy and hovering strategy, the optimal trajectory obtained by applying the ACO algorithm is shown in Figs. 8 and 9. It can be observed that compared with the trajectory determined by the GTO optimization method, the proposed GLC-AEM algorithms returns a trajectory at a much lower flying altitude. The UAV station is therefore deployed closer to the target MTCDs, which results in more favorable channel condition for data collection from the EE perspective. This is validated by the results shown in Fig. 10. Specifically, the proposed GLC-AEM algorithm on average reduced the energy consumption by about 23% compared with the GTO method.

In Fig. 10, we compare the GLC-AEM algorithm proposed in this paper with the hybrid hovering positions selection (HHPS) algorithm in [16] from the energy efficiency perspective. The HHPS uses k-medoids clustering method to cluster the ground MTCDs and determine the hovering point of the UAV. Then the traveling salesman problem for optimal UAV flying route determination is solved by a heuristic algorithm. Compared with the HHPS algorithm, the proposed GLC-AEM algorithm reduced the energy consumption by about 18%. This is because the HHPS algorithm does not return an optimized in-cluster hovering point of the UAV after clustering. As the number of MTCDs increases, the MTCDs' average energy consumption achieved by the GTO, HHPS and GLC-AEM algorithms is monotonically decreasing. This can be explained by the fact that the UAV's maneuvering energy consumption is larger compared with that for communications. But when the number of MTCDs increases, the average UAV maneuvering energy consumption per-served-MTCD gradually decreases.

Finally, we examine the performance of the proposed scheme in the multi-UAV scenario for data collection in clustered mMTC networks. The MTCD clustering and UAV hovering strategies are determined by the CND and GLC-AEM algorithms, which is the same as in the single UAV case. The flying paths of multiple UAVs are determined by solving a multiple traveling salesmen problem with the ACO algorithm. Simulation results in Fig. 11 show that as the number of UAVs increases, the mission time is significantly reduced, which is favorable for delay-sensitive tasks. However, the UAVs' maneuvering energy consumption increases with the number of UAVs, resulting in an increase in the per-MTCD energy consumption. Therefore, when the data to be collected from the mMTC network is delay-insensitive in nature, it is more desirable to use a single UAV station from the energy efficiency perspective.

Authorized licensed use limited to: UNIVERSITY OF VICTORIA. Downloaded on January 26,2023 at 04:32:29 UTC from IEEE Xplore. Restrictions apply.

Assuming that there are three UAVs. In Fig. 12 we show an example of the 3-D UAV trajectories obtained by the proposed GLC-AEM algorithm, where $K = 200$, and $L = 15$ were used in the simulation. Specifically, the GLC-AEM algorithm determines the optimal UAV hovering positions in the 3-D space. After that, the 15 cluster heads are subdivided into 3 groups by applying the K-means algorithm, corresponding to the mission areas of the 3 UAVs, respectively. The flying trajectory of each UAV is a closed-loop that can be obtained by applying the ACO algorithm.

VII. Conclusion

This paper has studied energy-efficient design of UAV-enabled data collection for mMTC networks. The problem of minimizing the total energy consumption for data collection has been formulated. It has been shown that as long as the flying altitude of the UAV is greater than its service radius multiplied by a constant, i.e. $h_a > \sqrt{3}r_{\max}$, there always exists an optimal trajectory that can be found by solving a global trajectory optimization (GTO) problem. However, the wireless channel deteriorates as the UAV flies at a relatively high altitude and thereby hurts the communication efficiency. Then, the AEM principle has been introduced as a new modeling method based on evaluation of an artificial energy function. The AEM-based modeling uses clustering technique to shorten the distance between UAV and MTCDs, which can effectively improves the overall energy efficiency. The overall energy consumption minimization problem for joint MTCD clustering and UAV trajectory design turned out to be a coupled non-convex problem that is challenging to solve. The optimization problem has been decomposed into two sub-problems by decoupling the flying variables and the other design variables. Then, the sub-problems deal with clustering-hovering optimization and inter-cluster flying trajectory optimization separately. Two algorithm, namely the CND and GLC-AEM, have been proposed to solve the MTCD clustering and in-cluster hovering position optimization problems through an iterative alternating optimization procedure. The second sub-problem has been transformed into a traveling distance minimization problem, which is readily solved by the ACO algorithm. Simulation results have shown that the GLC-AEM algorithm is applicable to both the single-UAV and multi-UAV data collection systems, and it can effectively reduce the system's energy consumption. Besides, the GLC-AEM algorithm has good scalability and better energy efficiency can be achieved when more MTCDs should be served.

Appendix

We first prove the convexity of the objective function in (8).

$$G = \sum_{k=1}^{K}\sum_{n=1}^{N} P_k(t_n)\tau + \sum v\tau_f \frac{m_{\rm v} g}{\eta_{\rm m}\eta_{\rm p}}. \tag{A.1}$$

In the above (A.1), $\sum v\tau_f$ is equivalent to the total distance the UAV travels. Let $d(t_n)$ denotes the distance between two adjacent hovering positions. Eqn. (A.1) is transformed into

$$G = \sum_{k=1}^{K}\sum_{n=1}^{N} P_k(t_n)\tau + \sum \frac{m_{\rm v} g}{\eta_{\rm m}\eta_{\rm p}} d(t_n). \tag{A.2}$$

Hence, the convexity of G depends on the second order derivative of $d(t_n)$.

$$\frac{\partial^2 d(t_n)}{\partial u^x(t_n)^2} = \frac{(u^y(t_{n+1}) - u^y(t_n))^2}{[(u^x(t_{n+1}) - u^x(t_n))^2 + (u^y(t_{n+1}) - u^y(t_n))^2)]^{\frac{3}{2}}}. \tag{A.3}$$

$$\frac{\partial^2 d(t_n)}{\partial u^y(t_n)^2} = \frac{(u^x(t_{n+1}) - u^x(t_n))^2}{[(u^x(t_{n+1}) - u^x(t_n))^2 + (u^y(t_{n+1}) - u^y(t_n))^2)]^{\frac{3}{2}}}. \tag{A.4}$$

$$\frac{\partial^2 d(t_n)}{\partial u^x(t_n)\partial u^y(t_n)} = \frac{\partial^2 d(t_n)}{\partial u^y(t_n)\partial u^x(t_n)} = \frac{-(u^x(t_{n+1}) - u^x(t_n))(u^y(t_{n+1}) - u^y(t_n))}{[(u^x(t_{n+1}) - u^x(t_n))^2 + (u^y(t_{n+1}) - u^y(t_n))^2)]^{\frac{3}{2}}}. \tag{A.5}$$

Based on (A.3), (A.4) and (A.5), the Hessian matrix of $d(t_n)$ is therefore written as

$$\bigtriangledown^2 d(t_n) = \begin{bmatrix} \frac{\partial^2 d(t_n)}{\partial u^x(t_n)^2} & \frac{\partial^2 d(t_n)}{\partial u^x(t_n)\partial u^y(t_n)} \\ \frac{\partial^2 d(t_n)}{\partial u^y(t_n)\partial u^x(t_n)} & \frac{\partial^2 d(t_n)}{\partial u^y(t_n)^2} \end{bmatrix}. \tag{A.6}$$

From (A.3), (A.4), (A.5) and (A.6), it is straightforward to show that $\frac{\partial^2 d(t_n)}{\partial u^x(t_n)^2} \geq 0$, $\frac{\partial^2 d(t_n)}{\partial u^y(t_n)^2} \geq 0$, $|\bigtriangledown^2 d(t_n)| = 0$. Therefore, $\bigtriangledown^2 d(t_n)$ is semi-definite positive. The convexity of the objective function G is verified based on the second-order condition of the function.

Next, we show that constraint (8b) is convex as long as the UAV's flying altitude is greater than its service radius multiplied by a constant. Define $r_{\max}$ as the maximum possible serving radius of the UAV in the data collection process. We prove that problem $\mathbf{P1}$ has a global optimal UAV flying trajectory as long as $h_a \geq \sqrt{3}r_{\max}$,

$$r_{\max} = \max\left\{\sqrt{(u^x(t_n) - q_k^x)^2 + (u^y(t_n) - q_k^y)^2}\right\},$$

$$\forall k = 1, \ldots, K, n = 1, \ldots N.$$

Proof: Let $z_k(t_n) = 1 + \frac{P_k(t_n)(\Pr_{\rm L}(t_n) + (1 - \Pr_{\rm L}(t_n))\kappa)}{\beta_0\sigma^2\|\mathbf{q}_k - \mathbf{u}(t_n)\|_2^2}$. If $z_k(t_n)$ is concave and positive, $\log(z_k(t_n))$ is concave. As a result, constraint (8b) is convex. Let $c = P_k(t_n)(\Pr_{\rm L}(t_n) + (1 - \Pr_{\rm L}(t_n))\kappa)/\beta_0\sigma^2$. Assuming that $P_k(t_n)$ and $\Pr_{\rm L}(t_n)$ does not change when optimizing the UAV's flying trajectory. Then c could be considered as a constant and as a result only the concavity of $z_k(t_n)$ needs to

Authorized licensed use limited to: UNIVERSITY OF VICTORIA. Downloaded on January 26,2023 at 04:32:29 UTC from IEEE Xplore. Restrictions apply.

be proved.

$$\frac{\partial^2 z_k(t_n)}{\partial u^x(t_n)^2} = \frac{8c(u^x(t_n)-q_k^x)^2-2c(h_a^2+(u^x(t_n)-q_k^x)^2+(u^y(t_n)-q_k^y)^2)}{(h_a^2+(u^x(t_n)-q_k^x)^2+(u^y(t_n)-q_k^y)^2)^3}. \tag{A.7}$$

$$\frac{\partial^2 z_k(t_n)}{\partial u^y(t_n)^2} = \frac{8c(u^y(t_n)-q_k^y)^2-2c(h_a^2+(u^x(t_n)-q_k^x)^2+(u^y(t_n)-q_k^y)^2)}{(h_a^2+(u^x(t_n)-q_k^x)^2+(u^y(t_n)-q_k^y)^2)^3}. \tag{A.8}$$

$$\frac{\partial^2 z_k(t_n)}{\partial u^x(t_n)\partial u^y(t_n)} = \frac{\partial^2 z_k(t_n)}{\partial u^y(t_n)\partial u^x(t_n)} = \frac{8c(u^x(t_n)-q_k^x)(u^y(t_n)-q_k^y)}{(h_a^2+(u^x(t_n)-q_k^x)^2+(u^y(t_n)-q_k^y)^2)^3}. \tag{A.9}$$

From (A.7), (A.8) and (A.9), the Hessian matrix of $z_k(t_n)$ is

$$\bigtriangledown^2 z_k(t_n) = \begin{bmatrix} \frac{\partial^2 z_k(t_n)}{\partial u^x(t_n)^2} & \frac{\partial^2 z_k(t_n)}{\partial u^x(t_n)\partial u^y(t_n)} \\ \frac{\partial^2 z_k(t_n)}{\partial u^y(t_n)\partial u^x(t_n)} & \frac{\partial^2 z_k(t_n)}{\partial u^y(t_n)^2} \end{bmatrix}. \tag{A.10}$$

Let the first-order principal minors of $\bigtriangledown^2 z_k(t_n)$ be non-positive, we have

$$h_a^2 \geq 3(u^x(t_n)-q_k^x)^2-(u^y(t_n)-q_k^y)^2, \tag{A.11}$$

$$h_a^2 \geq 3(u^y(t_n)-q_k^y)^2-((u^x(t_n)-q_k^x)^2. \tag{A.12}$$

Then let the second-order principal minors be non-negative and obtain

$$h_a^2 \geq 3[(u^x(t_n)-q_k^x)^2+(u^y(t_n)-q_k^y)^2]. \tag{A.13}$$

Consequently, in order to guarantee concavity of $z_k(t_n)$, there must be $h_a \geq \sqrt{3}r_{\max}$. Therefore, we can obtain the optimal solution of $\mathbf{P1}$ given the above condition is satisfied. It is worth noting that $h_a \geq \sqrt{3}r_{\max}$ means that the elevation angle is greater than 60 degrees. According to [32], the occurrence probability of LoS is approximately equal to 1 when the elevation angle is greater than 60 degrees even in an urban environment. In this cases, the air-to-ground links can be viewed as LoS links. Therefore, the assumption that $\Pr_{\mathrm{L}}(t_n)$ is constant at the beginning of this proof is reasonable. ■

ACKNOWLEDGMENTS

This work was supported in part by the National Natural Science Foundation of China (NSFC) under grants 61771431 and 61801434, in part by the Open Research Fund of State Key Laboratory of Millimeter Waves under grant K202214, in part by the Henan Province Key Science and Technology Project under grant No. 202102210328, and in part by the Zhengzhou Major Projects of Scientific and Technological Innovation under grant No. 2020CXZX0080.

REFERENCES

[1] M. Kamel, W. Hamouda, and A. Youssef, "Uplink coverage and capacity analysis of mMTC in ultra-dense networks," *IEEE Trans. Veh. Technol.*, vol. 69, no. 1, pp. 746–759, Jan. 2020.
[2] B. Wang, Y. Sun, and X. Xu, "A scalable and energy-efficient anomaly detection scheme in wireless SDN-based mMTC networks for IoT," *IEEE Internet Things J.*, vol. 8, no. 3, pp. 1388–1405, Feb. 2021.
[3] S. K. Sharma and X. Wang, "Toward massive machine type communications in ultra-dense cellular IoT networks: Current issues and machine learning-sssisted solutions," *IEEE Commun. Surv. Tut.*, vol. 22, no. 1, pp. 426–471, Jan.–Mar. 2020.
[4] S. Horsmanheimo *et al.*, "Remote monitoring of IoT ssensors and communication link quality in multisite mMTC testbed," in *Proc. IEEE 30th Annu. Int. Symp. Pers., Indoor Mobile Radio Commun.*, 2019, pp. 1–7.
[5] S. R. Pokhrel, J. Ding, J. Park, O. S. Park, and J. Choi, "Towards enabling critical mMTC: A review of uRLLC within mMTC," *IEEE Access*, vol. 8, pp. 131796–131813, 2020.
[6] J. Huang, W. Zhan, X. Sun, P. Liu, and D. Kong, "Cluster-based group paging scheme with preamble reuse for mMTC in 5G nnetworks," in *Proc. IEEE Glob. Commun. Conf.*, 2020, pp. 1–6.
[7] K. Mikhaylov *et al.*, "Energy efficiency of multi-radio massive machine-type communication (MR-MMTC): Applications, challenges, and solutions," *IEEE Commun. Mag.*, vol. 57, no. 6, pp. 100–106, Jun. 2019.
[8] 3GPP TR 45.820, "Cellular system support for ultra-low complexity and low throughput Internet-of-Things (CIoT) (Release 13)," Nov. 2015.
[9] L. Shen, N. Wang, J. Xiang, X. Mu, and L. Cai, "Iterative trajectory optimization for physical layer secure buffer-aided UAV mobile relaying," *Sensors*, vol. 19, no. 15, pp 1–17, Aug. 2019.
[10] Y. Li, Y. Zhang, and L. Cai, "Optimal location of supplementary node in UAV surveillance system," *Elsevier J. Netw. Comput. Appl.*, vol. 140, pp. 23–39, Aug. 2019.
[11] Y. Li and L. Cai, "UAV-assisted dynamic coverage in heterogeneous cellular system," *IEEE Netw. Mag.*, vol. 31, no. 4, pp. 56–61, Jul.Aug. 2017.
[12] S. Zhang, H. Zhang, B. Di, and L. Song, "Cellular UAV-to-X communications: Design and optimization for multi-UAV networks," *IEEE Trans. Wireless Commun.*, vol. 18, no. 2, pp. 1346–1359, Feb. 2019.
[13] J. Miao, P. Wang, Q. Zhang, and Y. Wang, "Throughput maximization for multi-UAV enabled millimeter wave WPCN: Joint time and power allocation," *China Commun.*, vol. 17, no. 10, pp. 142–156, Oct. 2020.
[14] F. Zhou, N. Wang, L. Fan, G. Luo, and W. Chen, "Edge caching in multi-UAV-enabled radio access networks: 3D modeling and spectral efficiency optimization," *IEEE Trans. Inf. Signal Process. over Netw.*, vol. 6, no. 4, pp. 329–341, Apr. 2020.
[15] J. Zhao, J. Liu, J. Jiang, and F. Gao, "Efficient deployment with geometric analysis for mmWave UAV communications," *IEEE Wireless Commun. Lett.*, vol. 9, no. 7, pp. 1115–1119, Jul. 2020.
[16] K. Zhu, X. Xu, and S. Han, "Energy-efficient UAV trajectory planning for data collection and computation in mMTC networks," in *Proc. IEEE Globecom Workshops*, 2018, pp. 1–6.
[17] S. R. Sabuj, A. Ahmed, Y. Cho, K.-J. Lee, and H.-S. Jo, "Cognitive UAV-aided uRLLC and mMTC services: Analyzing energy efficiency and latency," *IEEE Access*, vol. 9, pp. 5011–5027, 2021.
[18] L. Shen, N. Wang, Z. Zhu, Y. Fan, X. Ji, and X. Mu, "UAV-enabled data collection for mMTC networks: AEM modeling and energy-efficient trajectory design," in *Proc. IEEE Int. Conf. Commun.*, 2020, pp. 1–6.
[19] Z. Wang, G. Zhang, Q. Wanga, K. Wangb, and K. Yang, "Completion time minimization in wireless-powered UAV-assisted data collection system," *IEEE Commun. Lett.*, vol. 25, no. 6, pp. 1954–1958, Jun. 2021.
[20] H. Hu, K. Xiong, G. Qu, Q. Ni, P. Fan, and K. B. Letaief, "AoI-minimal trajectory planning and data collection in UAV-assisted wireless powered IoT networks," *IEEE Internet Things J.*, vol. 8, no. 2, pp. 1211–1223, Jan. 2021.
[21] C. Mao, J. Liu, and L. Xie, "Multi-UAV aided data collection for age minimization in wireless sensor networks," in *Proc. Int. Conf. Wireless Commun. Signal Process.*, 2020, pp. 80–85.
[22] C. Zhan and Y. Zeng, "Completion time minimization for multi-UAV-enabled data collection," *IEEE Trans. Wireless Commun.*, vol. 18, no. 10, pp. 4859–4872, Oct. 2019.
[23] X. Lin, G. Su, B. Chen, H. Wang, and M. Dai, "Striking a balance between system throughput and energy efficiency for UAV-IoT systems," *IEEE Internet Things J.*, vol. 6, no. 6, pp. 10519–10533, Dec. 2019.
[24] Z. Wang, R. Liu, Q. Liu, J. S. Thompson, and M. Kadoch, "Energy-efficient data collection and device positioning in UAV-assisted IoT," *IEEE Internet Things J.*, vol. 7, no. 2, pp. 1122–1139, Feb. 2020.

Authorized licensed use limited to: UNIVERSITY OF VICTORIA. Downloaded on January 26,2023 at 04:32:29 UTC from IEEE Xplore. Restrictions apply.

[25] S. Yang, Y. Deng, X. Tang, Y. Ding, and J. Zhou, "Energy efficiency optimization for UAV-assisted backscatter communications," *IEEE Commun. Lett.*, vol. 23, no. 11, pp. 2041–2045, Nov. 2019.
[26] S. Fu *et al.*, "Energy-efficient UAV enabled data collection via wireless charging: A reinforcement learning approach," *IEEE Internet Things J.*, vol. 8, no. 12, pp. 10209–10219, Jun. 2021.
[27] L. Na, Y. Liu, L. Zhao, D. O. Wu, and Y. Wang, "An adaptive UAV deployment scheme for emergency networking," *IEEE Trans. Wireless Commun.*, vol. 21, no. 4, pp. 2383–2398, Apr. 2022.
[28] Y. Zeng, J. Xu, and R. Zhang, "Energy minimization for wireless communication with rotary-wing UAV," *IEEE Trans. Wireless Commun.*, vol. 18, no. 4, pp. 2329–2345, Apr. 2019.
[29] Y. Pan, X. Da, H. Hu, Z. Zhu, R. Xu, and L. Ni, "Energy-efficiency optimization of UAV-based cognitive radio system," *IEEE Access*, vol. 7, pp. 155381–155391, 2019.
[30] S. Bi, J. Lyu, Z. Ding, and R. Zhang, "Engineering radio maps for wireless resource management," *IEEE Wireless Commun.*, vol. 26, no. 2, pp. 133–141, Apr. 2019.
[31] S. Zhang and R. Zhang, "Radio map-based 3D path planning for cellular-connected UAV," *IEEE Trans. Wireless Commun.*, vol. 20, no. 3, pp. 1975–1989, Mar. 2021.
[32] A. Al-Hourani, S. Kandeepan, and S. Lardner, "Optimal LAP altitude for maximum coverage," *IEEE Wireless Commun. Lett.*, vol. 3, no. 6, pp. 569–572, Dec. 2014.
[33] S. Boyd and L. Vandenberghe, *Convex Optimization*. Cambridge, U.K.:Cambridge Univ. Press, 2004.

Lingfeng Shen received the B.Sc. degree in applied mathematics from Zhengzhou University, Zhengzhou, China, in 2016. He is currently working towards the Ph.D. degree in information and communication engineering with Zhengzhou University. From 2019 to 2020, he was a Visiting Ph.D. Student with the Department of Electronics and Computer Engineering, McMaster University, Hamilton, ON, Canada, and in 2018, he was a Visiting Ph.D. Student at the Department of Electronics and Computer Engineering, University of Victoria, Victoria, BC, Canada, . His research interests include wireless communications and networking, focusing on UAV communication, mobile edge computing, and machine learning.

Ning Wang (Member, IEEE) received the B.E. degree in communication engineering from Tianjin University, Tianjin, China, in 2004, the M.A.Sc. degree in electrical engineering from The University of British Columbia, Vancouver, BC, Canada, in 2010, and the Ph.D. degree in electrical engineering from the University of Victoria, Victoria, BC, Canada, in 2013. From 2004 to 2008, he was with the China Information Technology Design and Consulting Institute as a Mobile Communication System Engineer, specializing in planning and optimization of commercial mobile communication networks. From 2013 to 2015, he was a Postdoctoral Research Fellow with the Department of Electrical and Computer Engineering, The University of British Columbia. Since 2015, he has been with the School of Information Engineering, Zhengzhou University, Zhengzhou, China, where he is currently a Professor. He also holds adjunct appointments with the Department of Electrical and Computer Engineering, McMaster University, Hamilton, ON, Canada, and the State Key Laboratory of Millimeter Waves, Southeast University, Nanjing, China. His research interests include resource allocation and security designs of future cellular networks, channel modeling for wireless communications, statistical signal processing, and cooperative wireless communications. He was on the technical program committees of international conferences, including the IEEE GLOBECOM, IEEE ICC, IEEE WCNC, and CyberC.

Zhengyu Zhu (Senior Member, IEEE) received the Ph.D. degree in information engineering from Zhengzhou University, Zhengzhou, China, in 2017. From 2013 to 2015, he visited the Communication and Intelligent System Laboratory, Korea University, Seoul, South Korea, to conduct a collaborative research as a Visiting Student. He is currently an Associate Professor with Zhengzhou University. He has authored or coauthored more than 40 journal articles in the IEEE publications. His research interests include information theory and signal processing for wireless communications, such as B5G/6 G, intelligent reflecting surface, the Internet of Things, machine learning, millimeter wave communication, UAV communication, physical-layer security, convex optimization techniques, and energy harvesting communication systems. Since 2021, Dr. Zhu has been an Associate Editor for the *Journal of Communications and Networks*, *Wireless Communications and Mobile Computing*, and *Physical Communications*.

Wei Xu (Senior Member, IEEE) received the B.Sc. degree in electrical engineering and the M.S. and Ph.D. degrees in communication and information engineering from Southeast University, Nanjing, China, in 2003, 2006, and 2009, respectively. From 2009 to 2010, he was a Postdoctoral Research Fellow with the Department of Electrical and Computer Engineering, University of Victoria, Victoria, BC, Canada, where he was an Adjunct Professor from 2017 to 2020. He is currently a Professor with the National Mobile Communications Research Laboratory, Southeast University. He was a Distinguished Visiting Fellow of the Royal Academy of Engineering, U.K., in 2019. He has authored or coauthored more than 100 refereed journal articles in addition to 36 domestic patents and four U.S. patents granted. His research interests include information theory, signal processing, and machine learning for wireless communications. Dr. Xu was the recipient of best paper awards from a number of prestigious IEEE conferences, including IEEE GLOBECOM. He received the Youth Science and Technology Award of China Institute of Communications in 2019. He was an Editor for the IEEE COMMUNICATIONS LETTERS from 2012 to 2017. He is also an Editor for the IEEE TRANSACTIONS ON COMMUNICATIONS and a Senior Editor for the IEEE COMMUNICATIONS LETTERS.

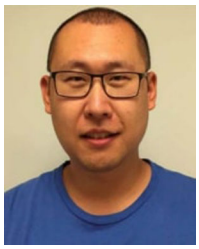

Yue Li received the Ph.D. degree in electrical and computer engineering from the University of Victoria, Victoria, BC, Canada, in 2018. From 2008 to 2013, he worked as a Standard Preresearch Engineer with the Wireless Research Department, Huawei, Shenzhen, China. He has been closely involved in 3GPP standards evolvement and has held numerous patents in WCMDA, LTE-A, and 5G systems. He is currently a Postdoctoral Research Fellow with the Department of Electrical and Computer Engineering, University of Victoria. His research interests include next-generation cellular systems, wireless network design and optimization, wireless system modeling, and performance analysis.

Authorized licensed use limited to: UNIVERSITY OF VICTORIA. Downloaded on January 26,2023 at 04:32:29 UTC from IEEE Xplore. Restrictions apply.

Xiaomin Mu received the B.S. degree from the Beijing Institute of Technology, Beijing, China, in 1982. She is currently a Professor Emeritus with the School of Information Engineering, Zhengzhou University, Zhengzhou. She has authored or coauthored many research papers in the field of communications and signal processing. She has also coauthored two textbooks. Her research interests include signal processing in communication systems, wireless communications, and cognitive radio networks.

Lin Cai (Fellow, IEEE) is a Professor with the Department of Electrical and Computer Engineering, University of Victoria, Victoria, BC, Canada. She is an NSERC E.W.R. Steacie Memorial Fellow, an Engineering Institute of Canada (EIC) Fellow, and an IEEE Fellow. In 2020, she was elected as a Member of the Royal Society of Canada's College of New Scholars, Artists and Scientists, and a 2020 "Star in Computer Networking and Communications" by N2Women. Her research interests include communications and networking, focusing on network protocol and architecture design supporting emerging multimedia traffic and the Internet of Things. She was a recipient of the NSERC Discovery Accelerator Supplement (DAS) Grants in 2010 and 2015, respectively. She has co-founded and chaired the IEEE Victoria Section Vehicular Technology and Communications Joint Societies Chapter. She is an Elected Member of the IEEE Vehicular Technology Society (VTS) Board of Governors, 2019–2024. She is the Associate Editor-in-Chief for IEEE TRANSACTIONS ON VEHICULAR TECHNOLOGY and has served as the Distinguished Lecturer of the IEEE VTS Society and IEEE ComSoc Society.

Authorized licensed use limited to: UNIVERSITY OF VICTORIA. Downloaded on January 26,2023 at 04:32:29 UTC from IEEE Xplore. Restrictions apply.